

Simulering av gassproduksjon i kullreservoar i Eclipse 100 og Tempest MORE

-Ei litteratur og casestudie av
metanproduksjon i kullreservoar

Jørgen Eikenes Dahle

Petroleumsfag

Innlevert: juni 2013

Hovedveileder: Jon Kleppe, IPT

Medveileder: Erik Nakken, Weatherford Consultants As

Noregs teknisk-naturvitskaplege universitet
Institutt for petroleumsteknologi og anvendt geofysikk

Preface

This master thesis was carried out during the spring 2013 for Weatherford Petroleum Consultants AS and NTNU with Professor Jon Kleppe as supervisor at NTNU and Erik Nakken as co-supervisor at Weatherford Petroleum Consultants AS. I would like to thank them both for their feedback and support during the work on this thesis.

I would like to thank reservoir engineer Knut Even Holter at Weatherford Petroleum Consultants AS, for many constructive hours with discussion and his feedback. I have no doubt that his experience with simulation and his patience with me as new to the software, has contributed heavily to the quality of this thesis.

I would like to thank my fellow students for five nice years on NTNU, with a social environment and room for learning. This final semester has been spent on Weatherford Petroleum Consultants AS premises, and I would like to thank the staff there for a warm welcome and a stimulating environment.

Lastly, I would like to thank my family for their support to me during my education, and for making my world a brighter one.

I hereby declare that the work on this thesis is made independently and in accordance with the rules set down by the Examination regulations made by the Norwegian University of Science and Technology, Trondheim.

Abstract

In this thesis I have done a literature study on coalbed methane, specifically on storage mechanisms, geology, transport mechanisms and sorption. The gas in coalbed methane is adsorbed onto the coal surface in micropores with a diameter of around 1×10^{-9} m. Even though the porosity of such coals is low, typically at 1-2%, the gas in place is huge, due to the gas being densely stored in the adsorbed state. The permeability of the coal matrix is miniscule, such that all gas production comes from the fracture system. As coal is brittle, such a fracture system will always be present, though the extent of it varies with the type of coal. I have found that the optimum coal for coalbed methane projects is the high volatile bituminous type B. At this rank, key parameters such as brittleness, coal retention and coal generation is most favorable. Investigation of the Langmuir isotherm, which describes the desorption of gas, was performed. I found that understanding it is key when doing a simulation and thus assessing the feasibility of a project.

Simulation of coalbed methane production in the mine Field-A was done in the simulators Eclipse 100 and Tempest MORE. There were several cases that were simulated. Permeability and desorption time was varied for a case with a single well and a simulation with five wells in a fivespot pattern was done. I found that due to the inherent differences between the two simulators the output gas rates were different as well. Eclipse 100 yielded larger gas rates consistently.

The simulation results obtained in this thesis have limited applicability as a means of evaluating the feasibility of a CBM project in Field-A. That is due to the limited number of wells in model used, not being able to fully capture the synergistic effect of multiple wells with short spacing in between.

“Simulation of coalbed methane production in Eclipse 100 and Tempest MORE”

Jørgen Eikenes Dahle

Trondheim, 21.06.2013

Sammendrag

I denne masteroppgåva har eg gjort ei litteraturstudie på gassproduksjon fra kull, der eg har sett nærare på korleis gassen er lagra og korleis den vert desorbert og så produsert. Gassen i kullforekomstar er adsorbert på overflata av kullet, i mikroporer som har ein diameter i størrelsesorden 1×10^{-9} m. Sjølv om porøsiteten i slike kull er låg, typisk 1-2%, så er gassinnholdet likevel høgt. Dette skuldes at gassen er tettpakka i adsorbert form. Permabiliteten i slike kull er låg, slik at for å produsere gass derifra må ein ha eit sprekkesystem som kan transportere gassen til brønnen. Sidan kull er sprøtt, er eit slikt sprekkesystem alltid tilstades, men kor stort eit slikt sprekkesystem er varierer med type kull. I denne oppgåva fann eg at av kull av typen «high volatile bituminous type B» er den kulltypen som egner seg best som gassproduserende kull. Dette fordi at denne er sprø, har evne til å holde på mykje gass og har generert mykje gass. Eg har undersøkt Langmuir isotermen, som brukast til å skildre korleis gass desorberes. Eg fann at det å forstå korleis forma på denne kurva virkar inn på gassproduksjonen er essensielt når ein skal gjere simuleringar og dermed evaluere mogelegheiten til å gjennomføre eit gassprosjekt i kull.

Eg gjorde simuleringar av gassproduksjon i kull i gruva Field-A i simulatorane Eclipse 100 og Tempest MORE. Fleire ulike scenario vart simulerte. Permabilitet og desorbsjonstid vart varierte for ein brønn for å sjå desse si effekt på resultatata. Eg simulerte og produksjon med fem brønnar i eit «fivespot» mønster. Eg fann at dei to simulatorane sine innebygde skilnader gav skilnader i resultatata som kom ut, sjølv om dataene dei brukte var like. Eclipse 100 gav generelt høgare gassrater enn Tempest MORE, men kor mykje høgare dei var varierte.

Resultata fra simuleringane har begrensa nytteverdi som verktøy for å evaluere om det er realistisk å produsere gass fra Field-A. Det skuldast at det er få brønnar (1 og 5) i simuleringane, slik at ein ikkje får sett synergieffektane av fleire brønnar som står tett saman.

Contents

Preface	2
Abstract	4
Sammendrag	6
List of figures	10
List of tables	12
Introduction	14
1 Litterature study	16
1.1 What is meant by unconventional and conventional gas production?.....	16
1.1.1 Conventional gas production	16
1.1.2 Unconventional gas production	16
1.2 Litterature study of coalbed methane	17
1.2.1 Introduction to coalbed methane	17
1.2.2 Economics of CBM	19
1.2.3 The geology of the coalbeds; Geologic history and the importance of coal rank ...	20
1.2.4 Porosity and storage capacity.....	26
1.2.5 Permeability and Cleat systems	28
1.2.6 Sorbtion- The key to understanding CBM production	31
2 Donetsk field in Ukraine- A case study	36
2.1 Background information on CBM in Ukraine.....	36
2.2 Geology of the Donetsk coal basin.....	37
2.3 The Field-A mine.....	40
2.3.1 Background information.....	40
2.3.2 Data acquisition on the field-A mine	40
3 Comparison of Tempest MORE and ECPLIPSE 100 on simulating the Field-A reservoir ..	44
3.1 A simple one layer, one well model.....	44
3.1.1 Description of Eclipse 100.....	44
3.1.2 Description of Tempest MORE and comparison to Eclipse 100	45
3.1.3 Simulation input.....	46
3.1.3.1 The first run: One vertical well	47
4 Results and discussion of the simulations.....	50
4.1 Results from the first run and discussion of these	50
4.1.1 Matching the results from MORE and Eclipse	50
4.1.2 Sensitivity studies of the first run.....	56

4.1.3 Simulation of a five spot pattern	63
4.2 Feasibility of field-A as a Coalbed methane project	67
5.0 Conclusion.....	70
List of symbols used.....	72
Bibliography	74
Attachments.....	76

List of figures

Figure 1: Text book illustration of production profile of a CBM well.....	18
Figure 2: Schematic of a typical production profile of a conventional gas well.....	18
Figure 3: Methane generated from coal, depending carbon content (Halliburton, 2007).....	22
Figure 4: Gas content of different ranked coals vs. pressure (Halliburton, 2007).	23
Figure 5: Unconfined compressive strength of coal by rank (Halliburton, 2007).....	24
Figure 6: Bed moisture versus carbon content. From (Halliburton, 2007).....	25
Figure 7: Visualization of micropores in coal. From (Halliburton, 2007).	26
Figure 8: Gas content comparison between conventional sandstone reservoirs and CBM reservoirs (Salsberry, Schafer, & Schraufnagel, 1996).	28
Figure 9: Figure showing diffusion of methane through the coal matrix (Salsberry, Schafer, & Schraufnagel, 1996).....	29
Figure 10: Typical relative permeability curves of a gas-water system in coal seams (Karimi & Pinczewski, 2005).....	31
Figure 11: Shape of a typical Langmuir Isotherm (Halliburton, 2007).....	34
Figure 12: Map showing the location of the Donetsk Basin, which Field-A and Field-B is part of (Triplet, Filippov, & Pisarenko, 2001).....	37
Figure 13: Detailed stratigraphy of the moscovian strata showing the suites of coal and their respective thicknesses (Sachsenhofer & Privalov, 2011).	39
Figure 14: Stratigraphy in the PM1 well in Field-B (Weatherford ASA, 2012).	42
Figure 15: Cumulative gas production in MORE and Eclipse.....	51
Figure 16: Gas production rate in MORE and Eclipse.....	51
Figure 17: Pressure in the reservoir in Eclipse at 1 January 2023	53
Figure 18: Pressure in reservoir in MORE at 1 January 2023.....	54
Figure 19: Cumulative water production in MORE and Eclipse.	55
Figure 20: Water production rate in MORE and Eclipse.	55
Figure 21: Gas (red) and water (green) production in MORE with $k=20$ mD, 20 year period. 57	
Figure 22: Gas production in MORE (red) and Eclipse (green) for $k=20$ mD, 20 year period 57	
Figure 23: Gas production in MORE with $K=5$ mD (red), 10 mD (green) and $K=20$ mD (blue) with simulation period of 100 years.	58
Figure 24: Gas production rate in MORE and ECLIPSE for $K=5$, 10 and 20 mD. MORE: 5 (blue), 10 (green) and 20 (red). Eclipse: 5 (purple), 10 (brown) and 20 (yellow).	59
Figure 25: Water production rate in MORE and Eclipse for $K= 5$, 10 and 20 mD. MORE: 5 (red), 10 (green), 20 (blue). Eclipse: 5 (purple), 10 (brown), 20 (yellow).....	59
Figure 26: Gas (red) and Water (green) production rate in MORE for $K=20$ mD, 100 year period.....	60
Figure 27: Gas rate in MORE for diffusion time= 2.5, 10, 50 and 100 days.....	62
Figure 28: Water production in MORE with diffusion time = 2.5 (red), 10 (green), 50 (blue) and 100 days (purple).	62
Figure 29: Gas production rate in Eclipse with $K=20$ mD and diffusion times at 2,5 (purple), 10 (blue), 50 (green) and 100 days (red).....	63
Figure 30: Water production rate in Eclipse with $K=20$ mD and diffusion times at 2,5 (purple), 10 (blue), 50 (green) and 100 days (red).....	63
Figure 31: Screen shot of the five-spot pattern model in MORE.	64
Figure 32: Gas production rate in Eclipse for a five-spot pattern. The wells are P1 (red), P2 (green), P3 (blue), P4 (purple) and P5 (yellow).	65

Figure 33: Gas production rate in MORE for a five-spot pattern. The wells are WPRD (red), WPRD2 (green), WPRD3 (blue), WPRD4 (purple) and WPRD5 (yellow).....	65
Figure 34: Gas rate for the center well in a five-spot pattern for MORE and Eclipse, shown together with the corresponding single well cases. Five-spot MORE (red), Single well MORE (green), Five-spot Eclipse (blue) and Single well Eclipse (purple)	66
Figure 35: Water production rate for center well in MORE and Eclipse for five spot pattern and single well. MORE five spot (purple), MORE single well (blue), Eclipse five spot (red) and Eclipse single well (green).....	66
Figure 36: Cumulative cash flow for fivespot pattern case from Eclipse (blue) and MORE (red) with $K=20$ mD with a timespan of 20 years.....	68
Figure 37: Coal layers with depths and thicknesses in the Field-A mine. From (DTEK, 2012).	76
Figure 38: PVT data generated and visualized in MORE.	77
Figure 39: Matching of the langmuir isotherms.....	78
Figure 40: Relative permeability curves used in simulation. Visualization done in MORE.	78

List of tables

Table 1: Illustration of the the time value of money has on CBM profitability. 19

Table 2: Table relating coal rank to test parameters (Halliburton, 2007)..... 20

Table 3: Classification system of coals from low-mature Lignite to highly mature anthracite.
Table as specified in Standard D388-88 by the Americal Society for Testing and Materials
(ASTM). 21

Table 4: Table showing various parameters effect on gas storage capacity. (Weatherford
Labs, 2012) 32

Table 5: Pressure difference in cells in MORE and Eclipse. 52

Introduction

Coalbed methane (CBM) has great potential in near future. The reserves of coal are large; estimates are at 13 trillion tons of high quality coal, distributed in 60 countries. Most CBM prospects are only in the test/pilot stage. The US was first in developing the coalbed methane resource, the first commercial CBM project was in Alabama in 1980 (Halliburton, 2007). Since then, the US has seen many more projects, and in year 2000 there were 13 986 wells in the country, producing some 105 MMSm³/day. Some other countries, like Australia and Canada have also developed CBM projects, but in most parts of the world where such projects are possible, they have yet to be undertaken. In Ukraine, this is the case. However, that is about to change. Ukraine is now looking to start CBM projects. Weatherford Petroleum Consultants have been hired to aid a local coal operator to start such a project, in the Field-A mine, located in the southeast of Ukraine. My simulations in this thesis will be done on a 20 km² virgin part of the field.

Methane as a resource is the most environmentally gentle of the petroleum resource family. Additionally, by producing methane before mining coal the hazards of the mining itself is reduced, as methane is explosive at concentrations higher than 5-15% in air (Halliburton, 2007). Further, methane is a highly efficient greenhouse gas, on a molecule-to-molecule basis the direct radiative effects of methane is 72 times stronger than that of carbon dioxide on a 20 year time scale (Forster et al. 2007). It has been estimated that 10% of the methane emissions to the atmosphere comes from coal mines. Thus, by producing and burning methane, thereby converting it to carbon dioxide, the radiative effects are significantly decreased (Halliburton, 2007).

Lastly, the utilization of production of methane from coalbeds substantially increases the natural gas base, and may thus be a crucial part of tomorrow's energy solution. In the US the estimated reserves of natural gas in CBM seams is 10000-25000 MMSm³, increasing the total gas reserves of the US by 50% (Halliburton, 2007). Undoubtedly, the future must hold a place for CBM projects!

A challenge with producing gas from coals is the low permeability and the water present in the coal seams initially. Together they give low gas rates initially, which is a challenge to the economic side of the project. Therefore, it is important to have knowledge of the reservoir prior to the decision of undertaking the project. A simulator is a helpful tool to attain such knowledge. Most simulators available are designed to simulate conventional reservoirs and the simulation of coalbeds being only available through "add-ons" to the simulators. As we shall see, the coal resource are quite different in some aspects than conventional sandstone or carbonate, this may pose a challenge to simulation of coals. One example of such

difference is the gas-water contact. In order to equilibrate the reservoir initially, simulators demand that the depth the gas-water contact (and other contacts if present) is given. But for coalbed methane projects this does not make sense, as the water is present in the fracture system, and gas in the matrix. This may be problematic if there are multiple layers in the model, as the fluids will move due to the density difference.

Different simulation tools have different solutions for coalbed methane simulation, in this thesis I investigated two such tools, namely Eclipse 100 and Tempest MORE. The goal is to see which solutions the simulators share, and where they differ. And how does this affect the output of the simulators. Several cases were simulated, one well with different permeabilities and desorption times and five wells in a fivespot pattern.

Additionally, the feasibility of a CBM project in the Field-A field was assessed.

The thesis is divided into two main parts, a literature study on CBM and a simulation part.

Due to the operator of the mine desiring discretion as to where the field is and the name of the fields in question, the fields will be termed field-A and field-B.

1 Literature study

1.1 What is meant by unconventional and conventional gas production?

1.1.1 Conventional gas production

By conventional gas production I mean gas production the way it has mostly been done in the past. Unconventional simply mean that something is new, it has not been done much before. The conventional gas reservoir is either in sandstone or carbonate. The conventional reservoir is best represented by a high single porosity model and usually has high permeability. That is very beneficial; as porosity relates to how much gas is present, and permeability to how fast it may be produced. The reason to why conventional gas reservoirs have such nice characteristics is simple, the oil industry started by producing gas where it was most profitable and technologically possible, thus making the beneficial cases conventional.

1.1.2 Unconventional gas production

By unconventional gas production one means simply gas production in reservoirs that one typically have been avoided in the past, due to their challenging nature. The challenge could be economical, technical, environmental or related to infrastructure, but more likely, a combination of these. But, due to less and less conventional reservoirs being found, unconventional reservoirs must be considered again. The reserves in unconventional reservoirs are huge, but the costs of producing them are often high as well, making the profitability of such projects vulnerable to downswings in the gas price. There are several types of fossil fuel projects that have recently become interesting to the industry, examples are shale gas, tight gas, heavy oil and *coalbed methane*.

This thesis is about simulation of coalbed methane in two different simulation tools, hence a deeper literature study of the characteristics of this resource is required. This will be done in the following chapter.

1.2 Literature study of coalbed methane

1.2.1 Introduction to coalbed methane

Over 60 countries have substantial coal reserves. In some places, like Eastern Europe, coal is indeed the only energy source available (Halliburton, 2007). Thus, CBM could prove a vital part of these countries future, both in terms of supplying energy and cleaner air. This is why most of the countries with coal deposits are now looking into CBM.

It can be stated that the methods of producing CBM is a merger between to schools, namely the oil- and coal industry. While methane had been produced on local scale from coal deposits previously, it was the oil industries' methods of fracking and dewatering, along with other methods, which brought methane production from coals up to a commercial level.

Production of coalbed methane is in some ways quite similar to conventional gas production, but also has some unique characteristics. Most notable, the coalbed reservoir has porosities ranging from 0,25-5% (Halliburton, 2007). Comparing to the porosities in conventional reservoirs of 15-40% this is little. Yet, pr. volume a coalbed methane reservoir may contain more gas than a conventional reservoir. This is seemingly a paradox, but it is explained by the fact that less than 10% of the gas in CBM reservoirs is stored in the primary porous area. The rest of the gas is stored in micropores, of only a few gas molecules width. In these pores the gas is adsorbed to the wall, instead of being in a free state like in the macropores of a conventional gas reservoir.

Prior to producing the gas the water in the natural fracture system must be produced, to enable the gas to flow. Also a critical pressure must be obtained, namely the desorption pressure P_{ds} , which is the pressure when water is saturated with methane and additional methane will go out of solution with water and create a two-phase flow regime. In other words, methane will only be produced *after* the desorption pressure is reached, hence a lot of water have to be produced before gas is recovered. Thus, the production profile of a CBM well looks quite different than that of a conventional gas well. The main difference is in the initial period, where conventional wells provide high rates from the start, while CBM wells see high water rates and low, but rising gas rates. This initial stage for CBM wells is termed dewatering stage. After the dewatering stage a plateau of gas production is reached, before the well see "normal" decline behavior. Rushing & A.D. Perego (2008) showed that normal decline curves from Arps original theory of 1945, may well be applied to CBM production as well.

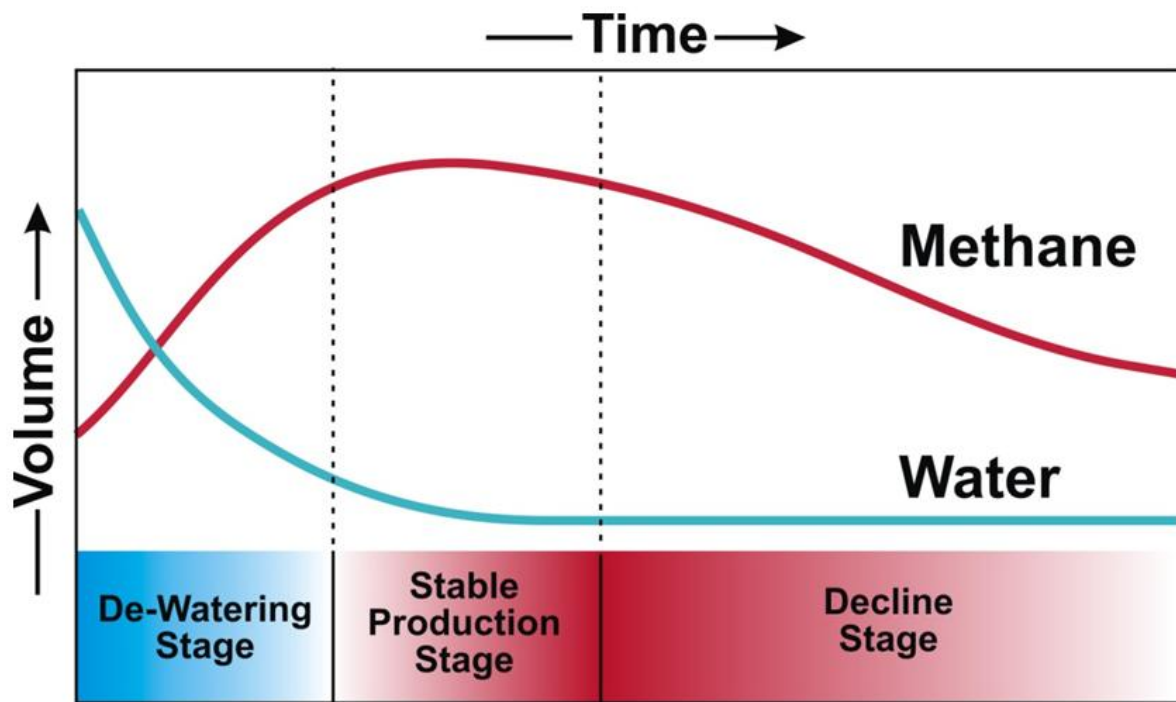


Figure 1: Text book illustration of production profile of a CBM well.

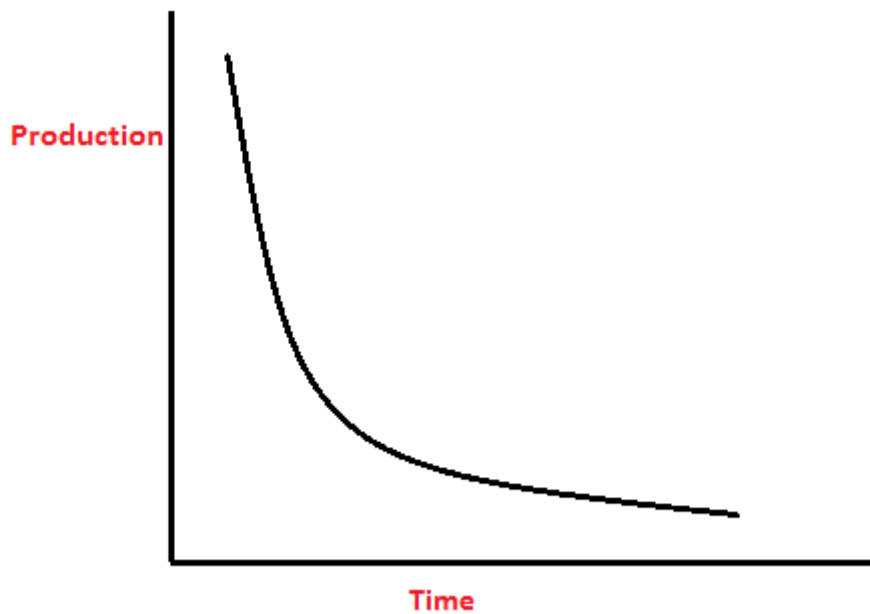


Figure 2: Schematic of a typical production profile of a conventional gas well.

1.2.2 Economics of CBM

The dewatering of the coal reservoir may take months or years, depending of the characteristics of a given reservoir. Needless to say, this is an economic challenge as the income from a CBM project is delayed compared to a conventional reservoir. In economic theory money today is far better than money later due to the time value of money. It is desirable to get return on invested money fast, as the internal rate of return devaluates the money earned in the future. Though companies demanded internal rate of return (IRR) are secret, it is usually somewhere between 10-16%. To illustrate this, let's use an IRR of 10% and assume the same gas production from a conventional and a CBM well, only the production from the CBM well is delayed by 2 years due to the mentioned dewatering. The declining production rates are random, but they serve well to illustrate as they are kept the same for the two well types. The results are shown in figure 3.

Table 1: Illustration of the the time value of money has on CBM profitability.

Years	Production [Sm3]		Value[USD in current money]	
	Conventional well	CBM well	Conventional well	CBM well
1	950		950.0	
2	900		818.2	
3	850	950	702.5	785.1
4	700	900	525.9	676.2
5	500	850	341.5	580.6
6	400	700	248.4	434.6
7	300	500	169.3	282.2
8	250	400	128.3	205.3
9	250	300	116.6	140.0
10	200	250	84.8	106.0
11		250	0.0	96.4
12		200	0.0	70.1
			4085.5	3376.5
IRR=	10 %			
Gas Price=	450 USD/1000 Sm3			

The impact of the delay on income is clear, as time goes the income generated dwindles due to the time value of money (through the high IRR). Percentage wise, the CBM well in this example would only generate 82% of the income of the conventional well, production rates and gas price being the same for both. This show the challenge related to income for CBM wells, which gives an incentive to innovate the process of dewatering. The shortening of the dewatering period is critical for CBM projects.

1.2.3 The geology of the coalbeds; Geologic history and the importance of coal rank

Certain critical parameters in CBM are highly dependent on a coal's geologic history and characteristics. Permeability depends on the cleat system of the coal, which in turn depend on the coals rank, e.g. its level of maturity, geologic events and stresses in the surrounding formation. The gas-in-place is highly dependent on coal rank; higher ranked coals produce more gas than lower ranked ones. Gas-in-place and permeability are perhaps the two parameters most critical to the success of a CBM project, or any gas project for that matter, as one indicates the value of the reservoir and the other the rate of which this value may be extracted. So, understanding of the geology is a necessity in order to determine a project's feasibility.

The formation of coal is started when plants are deposited in swamps and submerged rapidly enough to limit oxidation but at the same time allows for bacterial decomposition (Halliburton, 2007). This is called peatification. As time goes, and the peat is buried more and more deeply, the process of coalification commences. Coalification is a function of temperature, pressure, composition of organic matter and time, temperature being the most important. Depending on the value of the three mentioned parameters a coal will reach a certain degree of maturation. This degree of maturation is termed coal rank. The rank may be determined in several ways, depending on which way is most convenient, though a proximate analysis determining ash content, volatile content, fixed carbon content and moisture content is usual. Reflectance tests may also be used. Table 2 shows how coals are classified according to the test parameters mentioned. The "% daf" label means "dry ash free", e.g. the carbon content has been normalized after ash and moisture is neglected.

Table 2: Table relating coal rank to test parameters (Halliburton, 2007).

Rank	Maximum Reflectance (%)^a	Volatile Matter (%)	Fixed Carbon (% daf)^b	Carbon Content (% daf)^c
an	>3	2 to 8 ^b	>92	>92
sa	2.05 to 3.00	8 to 14 ^b	86 to 92	91 to 92
lvb	1.50 to 2.05	14 to 22 ^b	78 to 86	89 to 91
mvb	1.10 to 1.50	22 to 31 ^b	69 to 78	86 to 89
hvAb	0.71 to 1.10	>31 ^b 31 to 39 ^c	<69	81 to 86
hvBb	0.57 to 0.71	39 to 42 ^c		76 to 81
hvCb	0.47 to 0.57	42 to 47 ^c		66 to 76
sub	<0.47	>47 ^c		<66

Table 3: Classification system of coals from low-mature Lignite to highly mature anthracite. Table as specified in Standard D388-88 by the American Society for Testing and Materials (ASTM).

Class	Group	Abbreviation
Anthracitic	Meta-Anthracite	ma
	Anthracite	an
	Semianthracite	sa
Bituminous	Low Volatile	lvb
	Medium Volatile	mvb
	High Volatile A	hvAb
	High Volatile B	hvBb
	High Volatile C	hvCb
Subbituminous	Subbituminous A	subA
	Subbituminous B	subB
	Subbituminous C	subC
Lignitic	Lignite A	ligA
	Lignite B	ligB

As coal is maturing it will pass through the stages shown in table 3, starting with lignite going through Subbituminous and Bituminous and ending in Anthracite. Of course, a coal need not mature to the final stage of anthracite, how mature a coal become is foremost limited by the temperature it experiences. Associated with the ranks are certain degrees of volatile generation. Water and carbon dioxide are the first volatiles generated. They are generated when a coal reaches temperatures around 100 C, which would correspond to a coal rank in the early bituminous category. Methane generation becomes substantial at the rank of hvAb (Halliburton, 2007). If the coal matures further methane generation is rapid, the coal will actually generate more methane than it can retain itself. This is why conventional gas reservoirs may be found in the vicinity of mature coal formations, the coal is a productive source rock! If coal reaches the anthracite rank it might generate several hundreds of Sm^3/ton , see figure 3, while only retaining around 15-20 Sm^3/ton , see figure 4. As may be seen in figure 4 the difference in gas content of the different ranked coals is not great, and

though anthracite produces and retains the most gas, other parameters may influence the success of a CBM project more, making other ranks more favorable than anthracite.

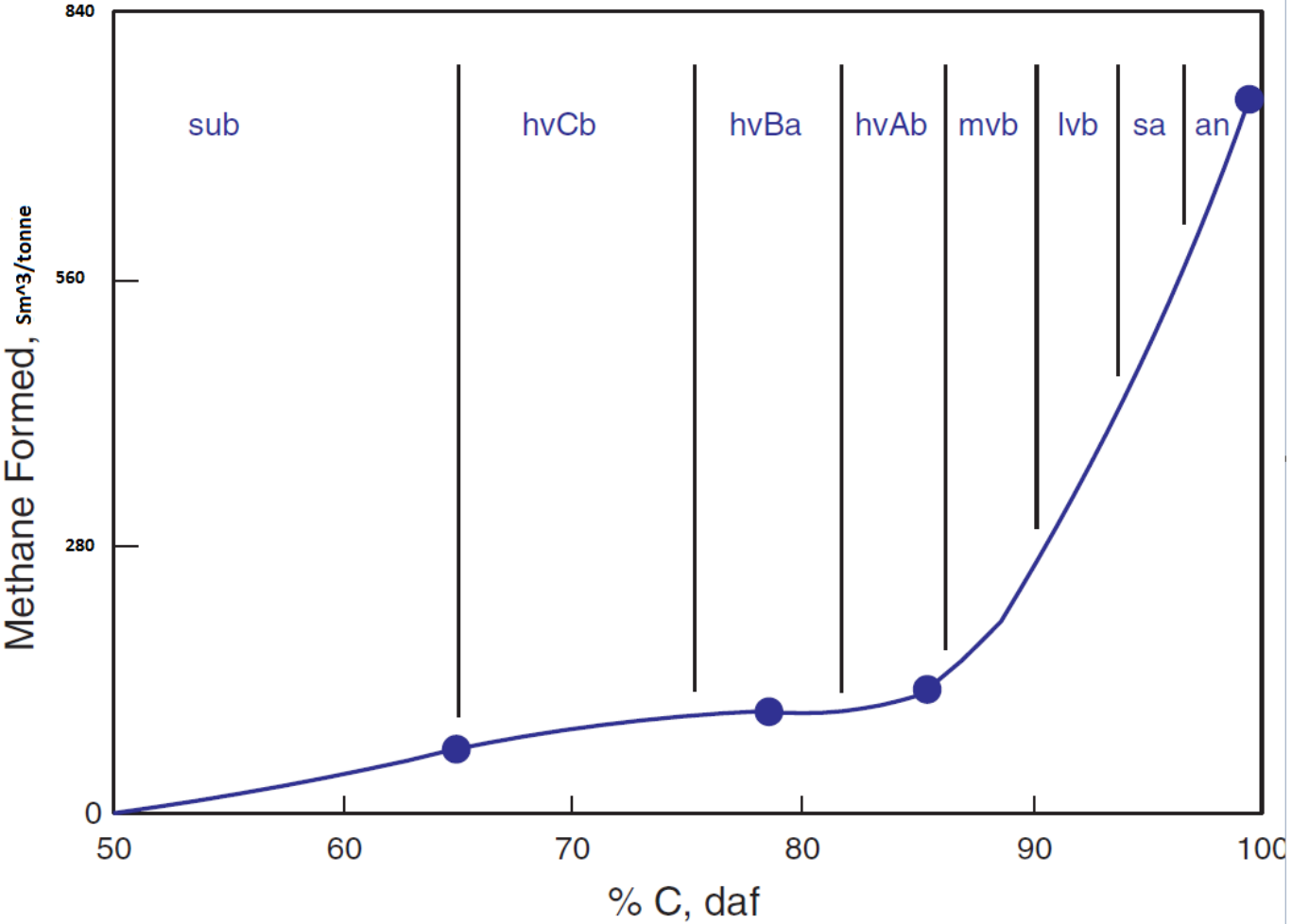


Figure 3: Methane generated from coal, depending carbon content (Halliburton, 2007).

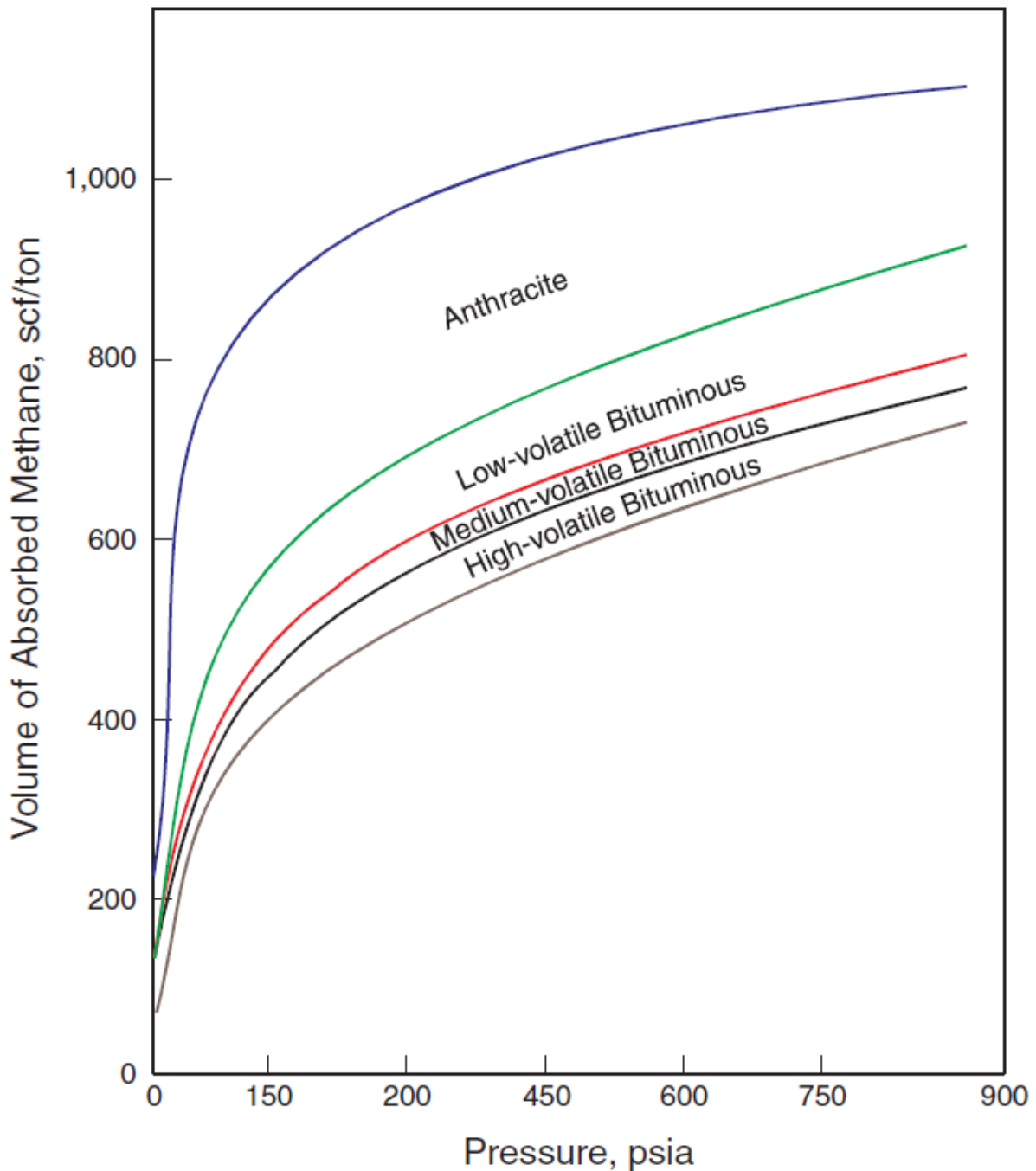


Figure 4: Gas content of different ranked coals vs. pressure (Halliburton, 2007).

Thus, even though the anthracitic rank generates most gas it is not the rank most sought after for CBM projects. As seen, the surplus gas generated migrates out of the coal anyway, and crucially; some key parameters are at an optimum at other ranks, namely the HvAb and Ivb subcategories of the bituminous rank.

One such parameter is the degree of fracturing of the coal. As coals have very little matrix permeability, fracture network permeability is crucial to the success of a CBM project. Indeed, the goal of a fracking completion would be to interconnect as many of the natural

fractures as possible. The compressive strength of coal varies with rank, reaching its minimum at a carbon-content corresponding to the rank high volatile, in the bituminous group. This is clear in figure 5, which shows the compressive strength of coal versus carbon content.

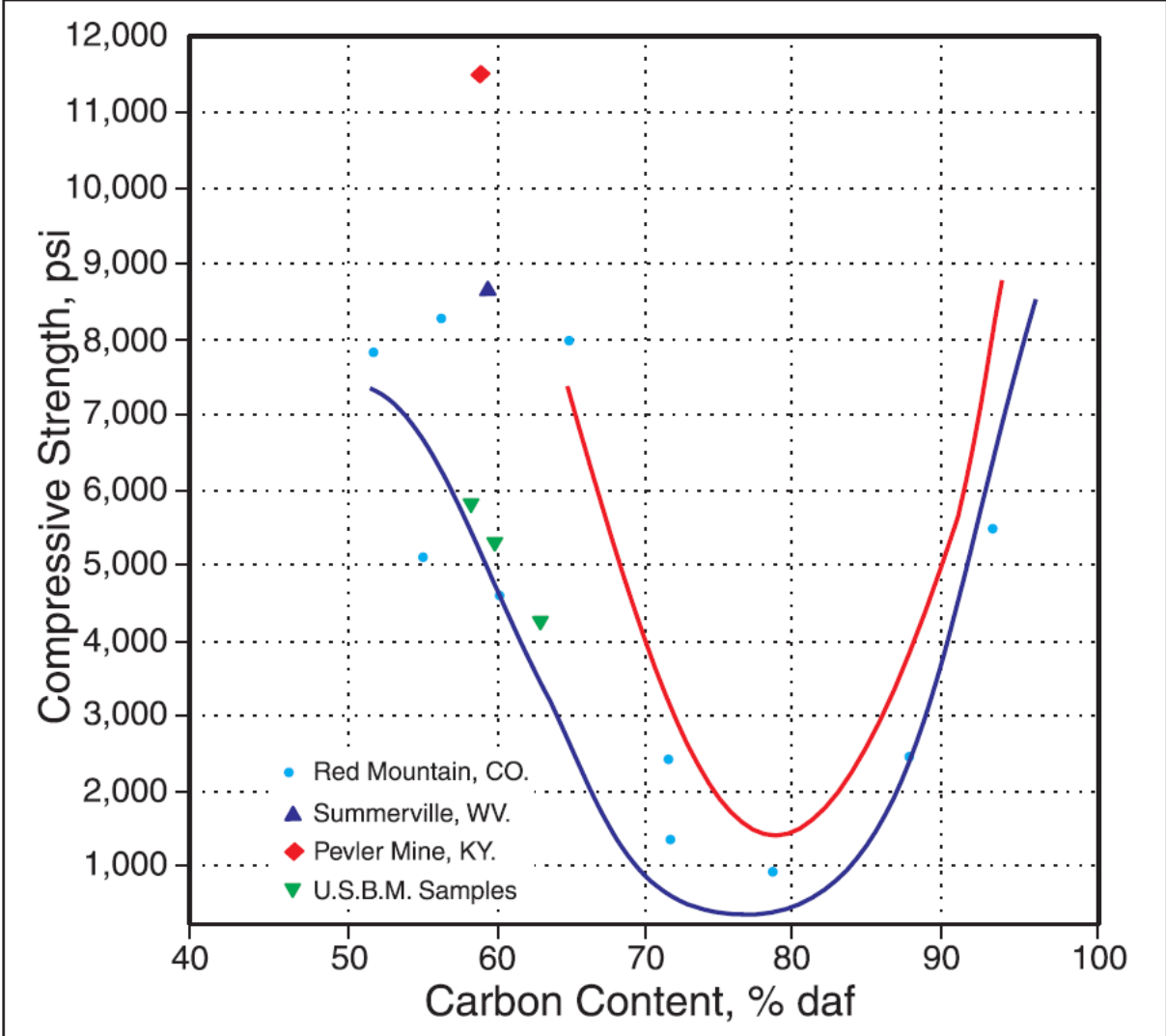


Figure 5: Unconfined compressive strength of coal by rank (Halliburton, 2007).

Low compressive strength in coal is favorable to the CBM project, as it makes the coal more brittle and fragile, and thus more prone to both natural and hydraulic fracturing and cavity completions.

The reason for the brittleness of the coals in the bituminous rank is that the coals shrink upon releasing volatiles, making them less ductile and more brittle. As a coal matures into the anthracitic rank the fractures created in the bituminous phase are closed, due to chemical processes such as molecular crosslinking reactions that bridge across the fractures (Halliburton, 2007).

The lower ranked coals have large bed-moisture contents. This would be unfavorable to the coal as a prospective CBM reservoir, as the bed-moisture reduces the adsorptive capacity of the coal for methane by occupying the available space in the micropores that methane otherwise could have adsorbed onto. This directly affects the coal ability to retain methane after it has been generated. The minima of bed-moisture content is to be found at a carbon content corresponding to the bituminous rank, subgroups m_{vb} and l_{vs}, as may be seen in figure 6.

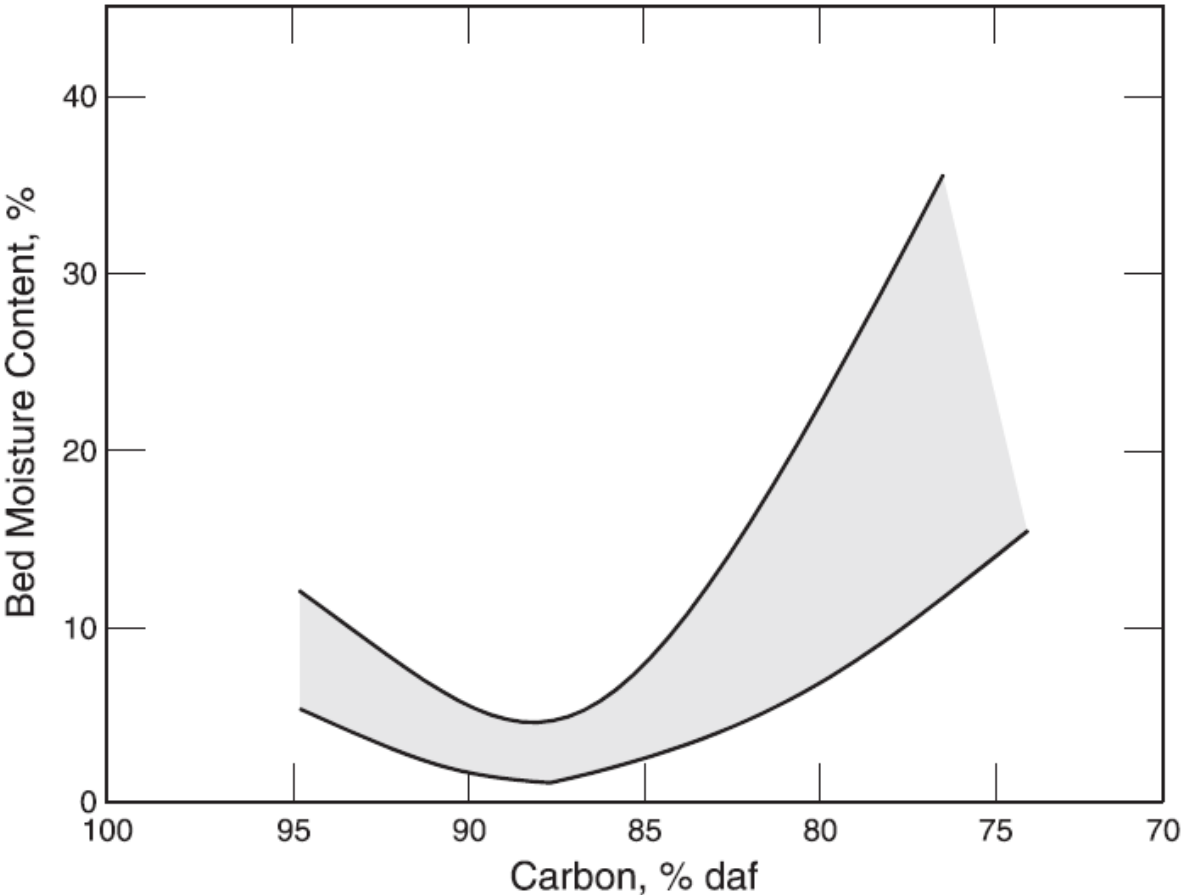


Figure 6: Bed moisture versus carbon content. From (Halliburton, 2007).

Bed-moisture, together with coal rank, pressure, ash and permeability of the coal and the surrounding formation determines the coals ability to retain methane. This is critical, because often the problem will not be that enough methane is not produced, but rather that it has migrated to somewhere else and is lost.

Bed-moisture must not be confused with free moisture, which is the moisture residing in the fracture system. It is this latter moisture that decreases relative permeability of gas by blocking the fracture system and therefore must be produced prior to gas production. The free moisture is not included in figure 6.

1.2.4 Porosity and storage capacity

A coal's storage capacity is of such nature that it may best be described by a dual porosity model. The matrix porosity, which is the volume of the micropores is the primary porosity, while the volume of the fractures is termed the secondary porosity.

The primary porosity is greatest in the low ranked coals. As the coal matures it is compressed with burial depth, volatiles are lost, and the micropores shrink. The primary porosity reaches its minima at the low volatile bituminous rank (Halliburton, 2007). The micropores are envisioned by Zwietering and van Krevelen in figure 7 (Halliburton, 2007).

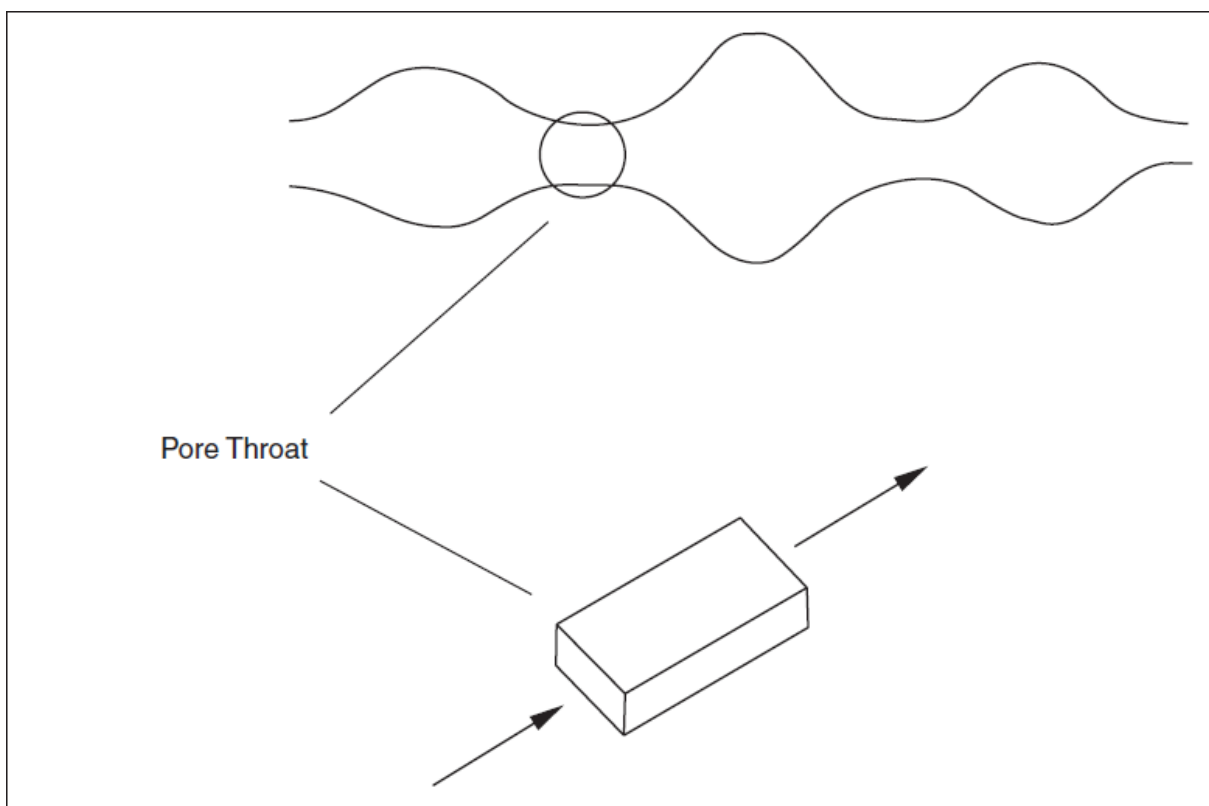


Figure 7: Visualization of micropores in coal. From (Halliburton, 2007).

As may be seen the coal consists of pore throats and pore cavities. The cavities' diameters are estimated to be 40 Å, e.g. 4×10^{-9} m, and the pore throats' diameter around 5-8 Å. These pore sizes are not uniform, and will change with rank. To put some perspective on the sizes mentioned it may be reminded of that a methane molecule's diameter is 3.5 Å, no wonder the matrix permeability in coals is low! Laboratory experiments suggest that alteration of the temperature may shrink these pore openings, at 77 K the pore throats shrink such that only helium may flow (Halliburton, 2007).

In some CBM wells heavier hydrocarbons have been found, such as the paraffins encountered in the San Juan basin, USA. These bigger molecules may block the pore throats. A solution to this was found in microbial injection, which resulted in increased methane production.

As mentioned earlier, the coal matrix shrink when volatiles are desorbed. But it may also go the other way around, if substances with strong adsorptive affinities, like carbon dioxide, contact the coal it may adsorb onto the coal and cause it to swell. This is detrimental to permeability as the pore throats would shrink.

Hence, the engineer working on a CBM project should pay attention to whether or not heavy hydrocarbons is part of the gas mix, temperature and the strong adsorptive gases.

The secondary porosity would be the porosity in the cleat systems. This includes the major fracture systems from the face and butt cleat systems, down to the smaller joints. These fracture systems are many times 100% saturated with water, and gas saturation is seldom more than 10% (Salsberry, Schafer, & Schraufnagel, 1996). The bulk porosity of the secondary porosity seldom exceeds 5%, this implies a very low storage capability for gas in the fracture system. It should be noted, that gas found in these systems are in the form of free gas, similarly to a conventional gas reservoir, while the rest of the gas is sorbed onto the matrix walls, and thus in adsorbed state. This implies that prior to the adsorbed gas being produced it must be desorbed, this will be more closely described in the chapter "sorption".

The fact that most of the gas is adsorbed on the matrix surface is what explains CBM reservoirs' high capability to store gas. The gas molecules are densely packed on the walls in layers (Halliburton, 2007), which is why coals with low porosity may hold higher gas amounts than sandstones of the same porosity at the same pressure. The surface area of the micropores in coals may be very large, reaching up to several hundred square meters per cubic centimeter, further explaining why coals may contain high amounts of sorbed gas (Triplett, Filippov, & Pisarenko, 2001). Figure 8 is a comparison of Gas-in-place values for sandstones at several porosities (10, 20, and 30%) and a CBM reservoir, at different pressures. Note that for low to medium pressures, the coals Gas-in-place exceeds even the gas-in-place of a sandstone with 30% porosity.

As may be seen in figure 8 the coals gas-in-place varies with pressure in a non-linear relationship. This relationship is best described by what is called the Langmuir isotherm (Salsberry, Schafer, & Schraufnagel, 1996) (Halliburton, 2007). The Langmuir isotherm must be determined for each specific coal, and varies highly with coal rank. It will be more closely described under "sorption", as it is obviously of high importance for a CBM projects potential.

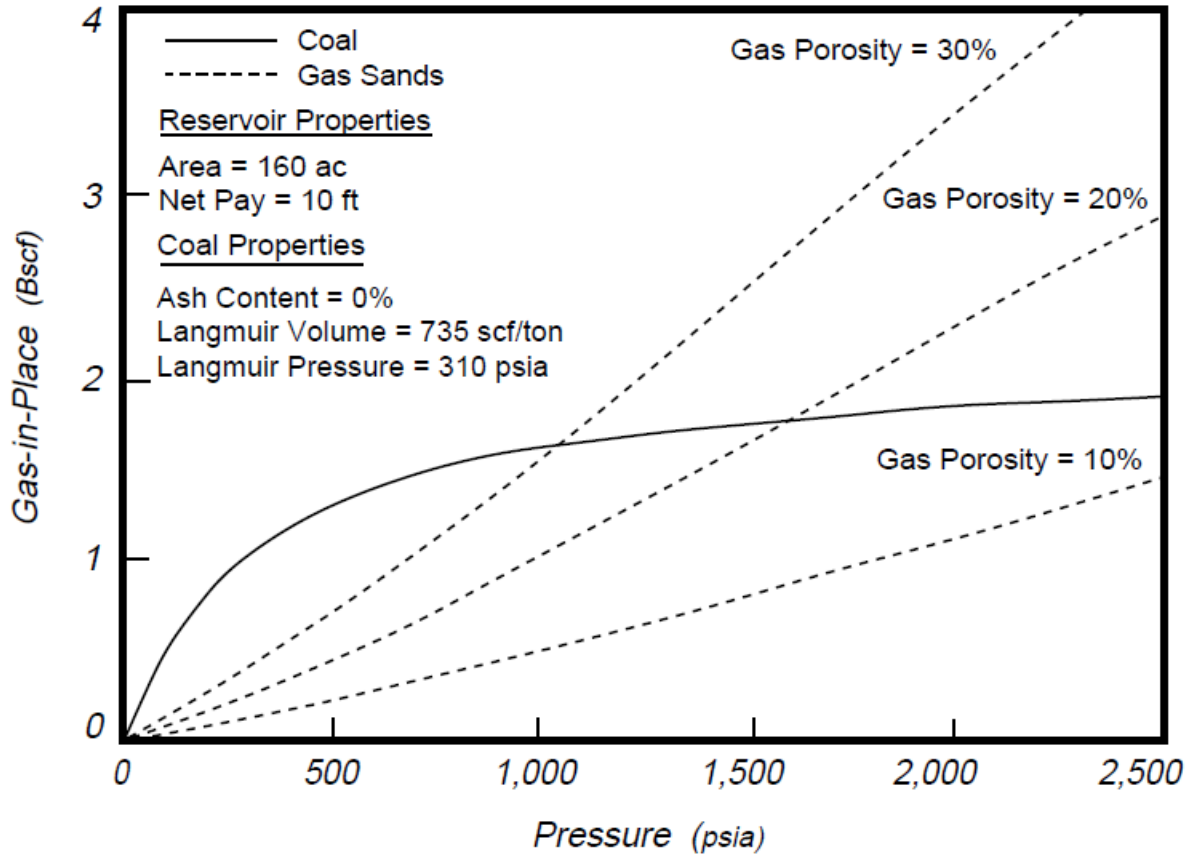


Figure 8: Gas content comparison between conventional sandstone reservoirs and CBM reservoirs (Salsberry, Schafer, & Schraufnagel, 1996).

1.2.5 Permeability and Cleat systems

Coals have very limited matrix permeability due to the very small diameter of the micropores. There the permeability is the microdarcy range, while the cleat system would exhibit permeabilities in the millidarcy range (Salsberry, Schafer, & Schraufnagel, 1996). For the gas to be produced, three processes must happen (Salsberry, Schafer, & Schraufnagel, 1996) (Halliburton, 2007);

- Desorption of methane from the coal matrix wall
- Diffusion of the methane through the matrix into the fracture system
- Transport of methane through the fractures to the well

Together the efficiency of these three processes determines the rate at which one might produce. The process of desorption is governed by the Langmuir isotherm and will be discussed further later. The diffusion of methane through the matrix is driven by the difference in concentration between the matrix micropores and the void in the fracture systems (Salsberry, Schafer, & Schraufnagel, 1996). This process is described by Fick's law

$$q_{gm} = \frac{8\pi DV_m}{S_f^2} (C_m - C(p)) \quad (1)$$

Where

q_{gm} is Gas production rate from the coal matrix, D is diffusion coefficient, V_m is matrix volume, S_f is fracture spacing, C_m is matrix gas concentration and $C(p)$ is equilibrium concentration at matrix-cleat boundary.

Note that fracture spacing, which of course is inversely proportional with fracture density, affects the production rate highly, as it is in the power of 2.

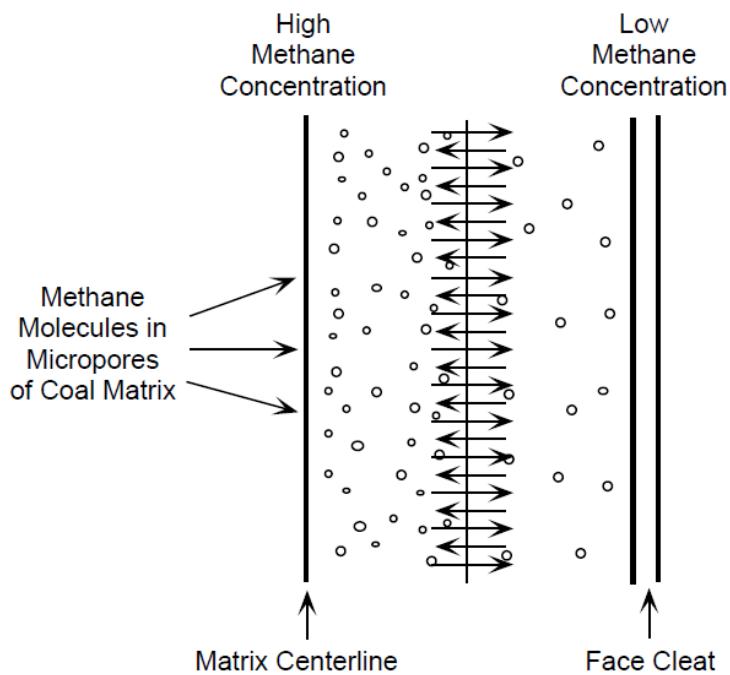


Figure 9: Figure showing diffusion of methane through the coal matrix (Salsberry, Schafer, & Schraufnagel, 1996).

Figure 9 illustrates the diffusion of methane through the coal matrix. The methane diffuses from the areas of high concentration to the low concentration cleat-matrix boundary.

Although the figure does not show this clearly, this diffusion happens through the small micropores. Depending on the geometry of the micropores and the pressure, some combination of Bulk diffusion, Knudsen diffusion and surface diffusion will take place.

As the methane has entered the fracture systems, the nature of its displacement changes. As with conventional gas production, its flow is governed by pressure gradients, in a manner which is described by Darcy's law (its general form):

$$Q = -\frac{kA}{\mu} \times \frac{\Delta P}{L} \quad (2)$$

Where

Q is flow rate, k is absolute permeability, A is the cross-sectional area of flow, μ is the fluids viscosity, ΔP is the pressure difference between two points, and L is the length between those points. As always, in flow governed by Darcy's law permeability is critical. In CBM reservoirs the permeability is dependent on the cleat systems, important parameters are cleat spacing, how many cleat systems which are present, and cleat aperture.

Thus, a closer description of the fracture systems, and how they influence permeability, is due. It is common to categorize the fracture systems into five types (Halliburton, 2007):

- Face cleats (primary)
- Butt cleats (secondary)
- Tertiary cleats
- Fourth-order cleats
- Joints

The face and butt cleats are the most important fracture systems as they impact permeability the most, but the others could also have a minor influence. Face cleats are the primary continuous fracture system found in coals. They are longer and have a wider aperture than the butt cleats, which they normally are perpendicular to. Anisotropic permeability is therefore often the case in CBM reservoirs. The directional permeability associated with the face cleat system may range from being the same as, or up to over 4 times larger than the permeability associated with the butt cleat system (Halliburton, 2007). This explains why the drainage area of a CBM well often will be elliptical, rather than circular. Typical values for permeability for the butt cleats may be 1-15 mD, and the face cleats may yield 1-50 mD.

The third- and fourth-order cleats are formed later than their primary and secondary counterparts, and thus terminate in them. These cleats will often stand at an angle of 45 degrees to the face and butt cleats. Not all CBM reservoirs have such high order fracture systems, but if present, they may boost permeability as was observed in the San Juan basin, USA (Halliburton, 2007).

Joints are fractures that run parallel to the face cleats. They form later though and are wider spaced apart. Joints may directly cross different layers, thus connecting them hydraulically. Thus, joints may improve vertical permeability.

Interestingly, the cleat spacing is present in two of the three transport processes that occur in CBM projects. It occurs directly in Fick's law and indirectly through permeability in Darcy's

law. One may conclude that it is paramount to determine the cleat spacing accurately before considering starting a CBM project, as it influences the rate of production so heavily.

In figure 10 a typical relative permeability plot for a coalbed methane system is shown. As may be seen the relative permeability of gas goes to 1 as the water saturation reaches 0.5-0.6. This plot emphasizes the importance of rapid dewatering, to enable the flow of gas.

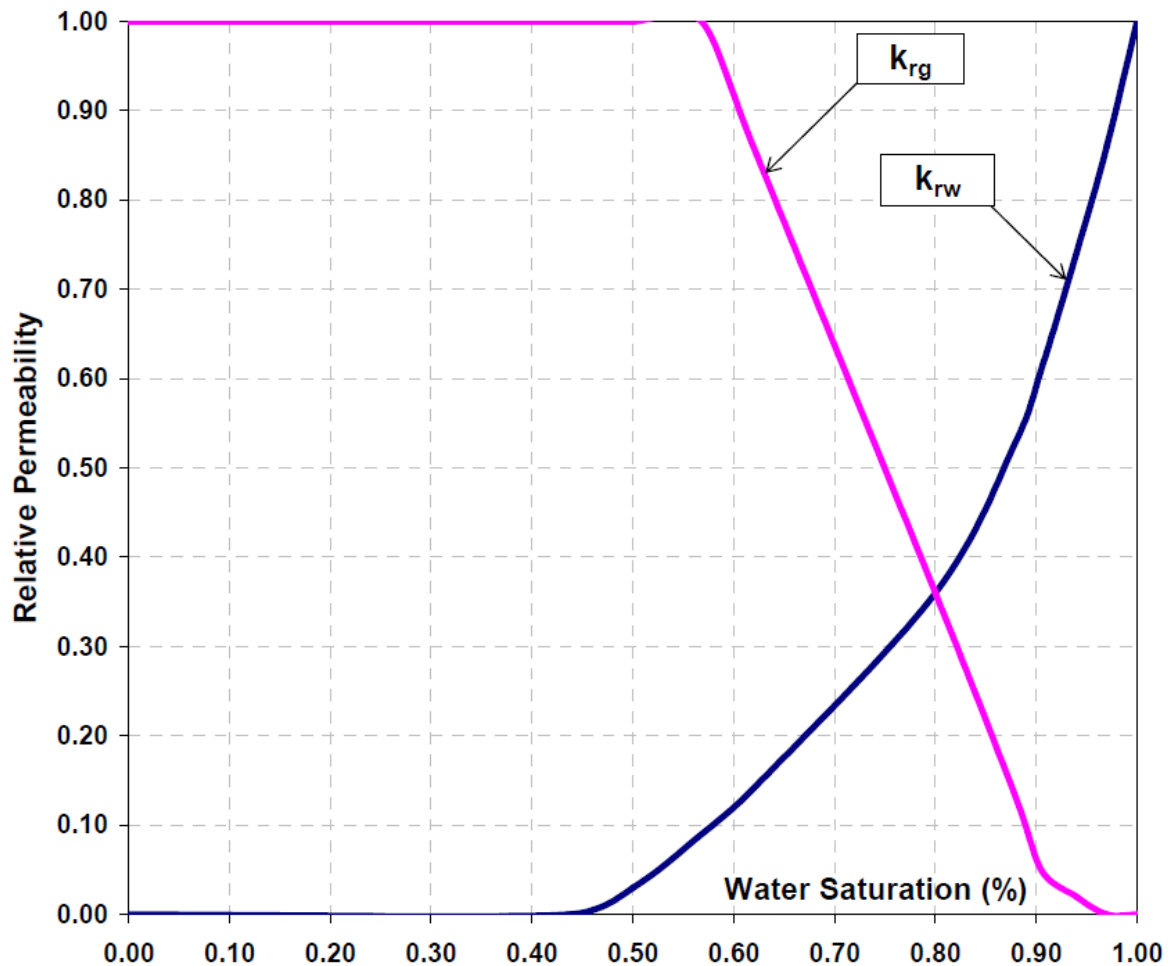


Figure 10: Typical relative permeability curves of a gas-water system in coal seams (Karimi & Pinczewski, 2005).

1.2.6 Sorption- The key to understanding CBM production

In coal bed methane reservoirs, the gas is stored rather differently than in normal sandstone or carbonate reservoirs. Whereas it is stored as free gas in the pores in the latter, it is densely packed on the surface of the micropores of the coal. The surface area of the micropores are actually immense, even though a typical diameter is of the order 1×10^{-9} m. Halliburton (2007) states that 1 pound of coal has the surface area of 55 football fields!

The nature of how the gas is stored in CBM reservoirs give rise to the need to describe and anticipate how fast, and at what pressure it will desorb from the coal. Through empirical studies a curve type has been found that matches the adsorption data of coals very well, it is called the Langmuir Isotherm. It relates the adsorbed gas volume to pressure, given a constant temperature. The shape of the curve is given by

$$V = \frac{V_L P}{P + P_L} \quad (3)$$

Where V is the volume of gas adsorbed, V_L is the langmuir volume, which is the maximum volume of gas the rock may adsorb, P is reservoir pressure and P_L is the Langmuir pressure, which is defined as the pressure where half of the gas has been desorbed (Weatherford Labs, 2012) (Roxar, 2012). Together, P_L and V_L give the shape of the isotherm. To make a match for an actual case, one simply manipulates P_L and V_L such that a match is obtained. Of course, an assessment of whether such an arbitrary match makes sense physically must be done.

In figure 11, an example of how such a curve may look is given. Note that at high pressures, little gas is adsorbed or desorbed at incremental pressure increase or decrease, while at lower pressure the same alteration would yield large changes in the amount of gas sorbed. This is noteworthy, as it means that bringing the reservoir pressure down low in CBM reservoirs is beneficial. There are practical limits exist as to how low the pressure may be brought, but it is feasible to inject nitrogen to lower the partial pressure of methane, to come even lower on the Langmuir isotherm.

Table 4: Table showing various parameters effect on gas storage capacity. (Weatherford Labs, 2012)

Parameters	As the Parameter:	Gas Storage Capacity:
Pressure	Increases	Increases
Temperature	Increases	Decreases
Moisture Content	Increases	Decreases
Vitrinite/Kerogen III Concentration	Increases	Increases
Thermal Maturity	Increases	Increases

In table 4 various parameters effect on gas storage capacity is given. Note that temperature and moisture increase is detrimental to the storage capacity. A higher thermal maturity, i.e. coal rank, and higher concentration of the mineral vitrinite yields an increase in gas storage capacity. This should be remembered when assessing whether or not a certain CBM project will be successful.

Initially, a reservoir may be undersaturated or, in rare cases oversaturated (Weatherford Labs, 2012). In the first case, the reservoirs real gas storage would be below the predicted one of the Langmuir isotherm. As the pressure then decreases, desorption would not occur until the pressure was reduced enough to bring the reservoir onto the Langmuir isotherm curve. The pressure at which this occurs is termed the critical desorption pressure, P_{ds} . It is an important parameters as it reveals when the first gas desorption, and thus production, will occur.

In the rare oversaturated case, gas would exist as free gas in the or gas dissolved in the moisture present in the fractures.

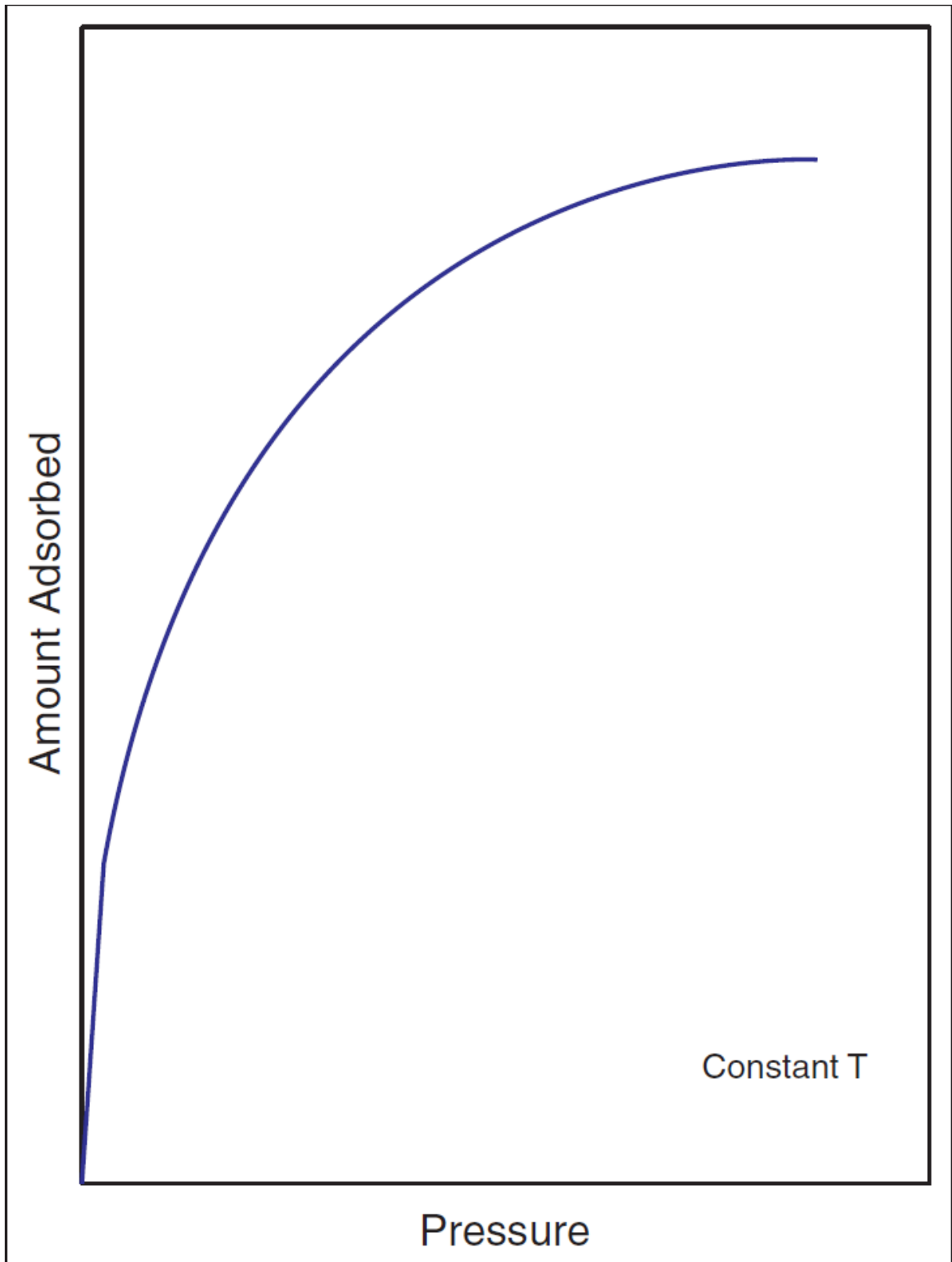


Figure 11: Shape of a typical Langmuir Isotherm (Halliburton, 2007).

2 Donetsk field in Ukraine- A case study

This section of the paper is dedicated to describing the Field-A mine in Ukraine. A description will be given on the geology in the region, with an emphasis on characteristics relevant for CBM projects. I will show how the Field-A mine fits into the theory on CBM given in chapter 1.2. Chapters 3 and 4 of this paper is about simulating the gas production from the named mine, so this section will also contain information about parameters that is relevant to such simulation.

2.1 Background information on CBM in Ukraine

There are several factors that make CBM projects attractive in Ukraine. The European Union is pressuring Ukraine to do something about the emissions of their coal mines. Large amounts of CO₂ is emitted from these mines, in 1999 2060 MMm³ of methane was released into the atmosphere from them (Triplett, Filippov, Pisarenko, & Blackburn, 2000).

The development of a CBM industry in Ukraine would also make the country less dependent on Russia for energy import. Currently, Ukraine has to buy gas from Russia at high prices, making for a trade deficit between the countries of over 2 billion dollars each year.

Finally, there is the issue of safety. The coal mines in Ukraine are a very hazardous place to work. If the concentration of methane exceeds 9 % pr. Volume it may explode. There have been many accidents due to this. In 1999, 296 workers lost their lives in the mines. To put this into perspective; in 2011, 168 people lost their lives in traffic accidents in Norway. This shows just how risky of a workplace the mines really are. The benefit of CBM projects is that they may synergize well with the coal mining. If the methane is drained prior to the coal being excavated the miners safety is improved. To make this happen, it is necessary to start methane production 10 years prior to coal mining, for a given area. So in order for the miners to benefit from CBM projects, virgin areas must be chosen. One such virgin prospect is the 20 km² area in the Field-A mine, that I will simulate coal methane production for in the next chapter.

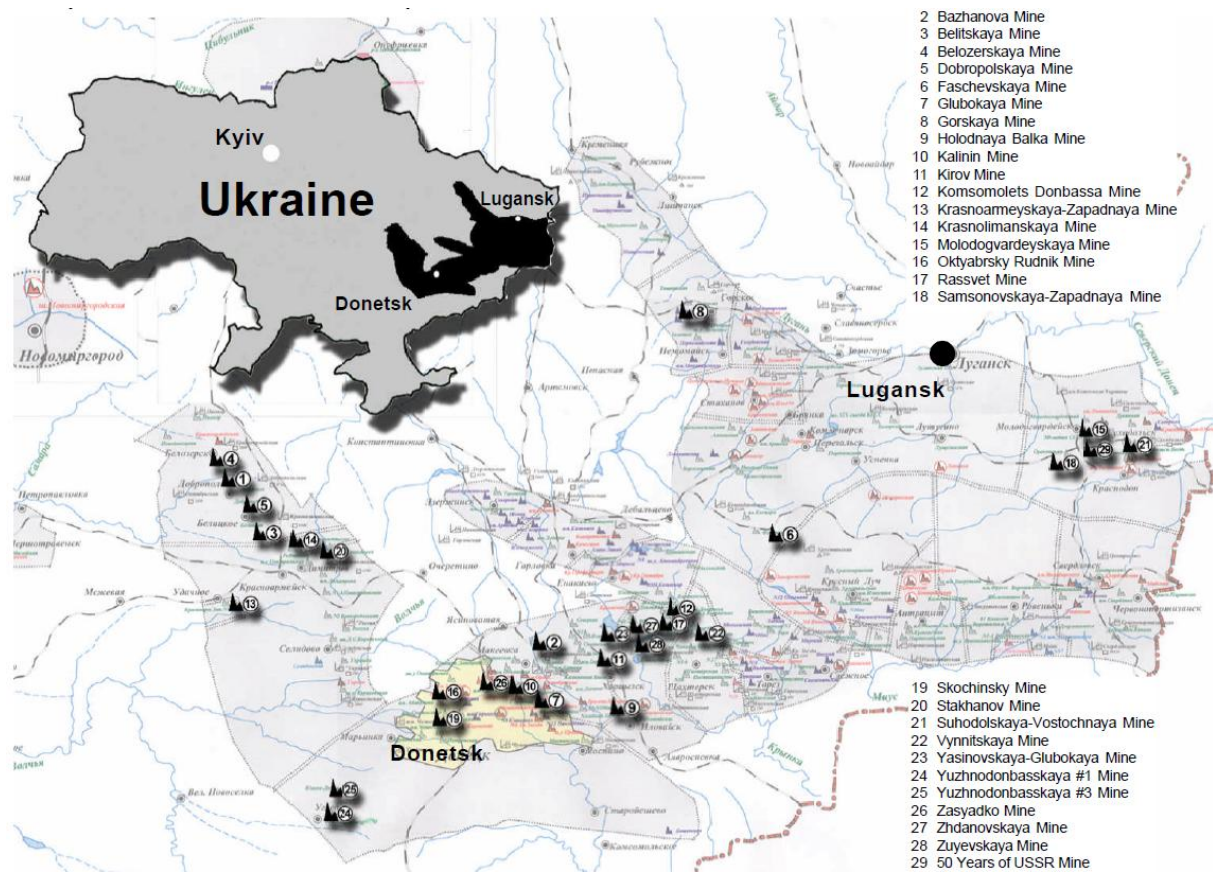


Figure 12: Map showing the location of the Donetsk Basin, which Field-A and Field-B is part of (Triplet, Filippov, & Pisarenko, 2001).

2.2 Geology of the Donetsk coal basin

The Donets Basin covers a huge area, around 60 000 km² (Sachsenhofer, et al., 2001). The known workable coal seams in the basin numbers around 130 (>0,45 m), which totals up to roughly 60 m (Sachsenhofer & Privalov, 2011), with an average seam thickness of 0,9 m (Sachsenhofer, et al., 2001). Although the seams are not thick, they are wide in lateral distribution, some of the seams extending throughout most of the entire field. The key strata are the Serpukhovian and the Moscovian stratas, they were deposited around 300-320 million years ago, in the carboniferous period (Sachsenhofer, et al., 2001). In figure 13 the Moscovian strata is shown. The coal seams are categorized into suites from a-z, from deepest to shallowest. Note how thin, but numerous the coal layers are. This presents a challenge when developing CBM projects, to obtain sufficient drainage when the gas is

stored in separate layers. A crucial question is then how large the vertical permeability is in the sand- and limestone layers in between the coal seams.

The coal seams of the Serpukhovian and Moscovian stratas contains high amounts of vitrinite, ash (12-18%) and sulfur (2,5-3,5%) (Sachsenhofer, et al., 2001). Most of the coal is of meta-anthracite rank. I refer to table 3, to remind that the meta-anthracitic rank is the most mature coal rank. This has some important implications. Firstly, the theory predicts that large volumes of gas have been generated in the coal seams, while much of this gas probably have dissipated and is lost, the miners in the area may testify to the fact that the coals are indeed very gassy. The average methane content is 14,7 m³/ton, although some places even exceeding 100 m³/ton. The high methane content is surely favoring the development of CBM projects in the area.

It is also interesting to look for conventional sandstone gas reservoirs in the vicinity of the meta-anthracitic coals. Considering the large discrepancy described in chapter 1.2 between methane generated and methane retained, it is likely that some of the surplus gas may have been trapped in some cases. The CBM developer should keep this in mind when drilling and logging, as undoubtedly the profitability of a project could be increased if crossproduction from neighboring gassy sands took place. Of course, the vertical permeability must be evaluated to ensure that crossflow actually will occur.

Depending on depth, the fluids in the coals vary. In the uppermost hundreds of meters, there is often a low concentration of CH₄. Instead, CO₂ and N are dominant. This zone is termed the gas weathering zone. Below follows a transition zone and then the methane zone. In the methane zone methane concentration may be well over 70 % (Not corrected for air based upon O₂ with H₂ removed) (Sachsenhofer & Privalov, 2011). When corrected for air, the methane concentration is typically around 90-98%, which conversely is a very clean hydrocarbon source.

2.3 The Field-A mine

2.3.1 Background information

The Field-A mine lies in the Donetsk region of Ukraine, as may be seen on the map in figure 12, and has been operational since 1980. It extends over an area of 62,5 km² and has 139 449 thousand tons of minable reserves left (numbers from 2001) (Triplett, Filippov, & Pisarenko, 2001). The coal seam gas content is in the range of 25-35 m³/ton (Triplett, Filippov, & Pisarenko, 2001). Triplett, Filippov, Pisarenko, & Blackburn (2000) states that the methane reserves are around 7 billion m³. However, the operator of the mine states that the potential is closer to 8 billion m³.

2.3.2 Data acquisition on the field-A mine

A problem when trying to simulate the virgin area in the field-A mine is the lacking of data. It has therefore been necessary to use data from elsewhere. There is a mine located in Field-B, around 80 km away from the field-A mine, where data is available. An end of well report written by Weatherford ASA is available, as well as lab results for coring samples taken in Field-B. These data are from a well called PM1, which is drilled into the d₄ coal seam at around 850-860 m depth (Weatherford ASA, 2012). Comparing with the virgin area in Field-A and the coal seam I have chosen for more detailed studies there, there are not great differences. However, the difference in age should be noted. The d₄ seam is older than the l₇ I have chosen, which also means a difference in depth. The l₇ lies shallower than the d₄, some hundred meters. This might give a difference in coal rank. It would probably only be marginal, as the depth difference is not great. However, it is possible, that some geologic event prior to the deposition of the l₇ layer was deposited matured the d₄ layer further such that some greater difference in coal rank could occur. The cores taken in the PM1 well in Field-B suggest a rank of medium-volatile bituminous rank.

The operator of the field-A mine states that the coal is towards semi-anthracitic rank, however, Triplett, Filippov, & Pisarenko (2001) states that the coal is more towards low-volatile bituminous. It seems strange that the shallower l₇ seam should be more mature than the deeper d₄ seam. Some geological event might be the reason for this, but that is beyond the scope of this thesis.

The l₇ have a slight dip and is largely continuous in the field-A area. There are plans to mine it from the depths of 808 to 401 m below ground. See figure 37 for details on the dip and geometry of the seam. Since the stratigraphy is quite similar to the field-A mine, I assume the data from field-B to be usable. These data include gas content, permeability, information on sand- and limestone, Langmuir isotherm.

In the Field-A mine there are alternating layers of sandstone, clay, coal and limestone. Some shale is also present together with the mentioned facies. Since proper logs are lacking for the area I will use the logs from Field-B as a means of illustrating the stratigraphy, assuming they are representative.

In the literature two coal stratums are highlighted as interesting, C₂⁶ and C₂⁷. These stratums contain 17 and 23 coal seams respectively. In the C₂⁶ stratum, five are deemed minable; l₇, l₃, l₆, l₁, and l₄. The average thickness of these are 0,96 to 1,38 m (Triplett, Filippov, & Pisarenko, 2001) and the depth of mining is in the range of 418-790 m.

In the C₂⁷ stratum four seams are deemed minable; m₉, m₅, m₄ and m₃. The average thickness ranges from 0,65 to 0,87 m (Triplett, Filippov, Pisarenko, & Blackburn, 2000).

The geothermal gradient is 2,3 C/100 m with an average temperature of 17,6 C at 100 m. And the pressure gradient is 6-12 MPa/1000 m with a gas pressure in surrounding rock of 4-8 MPa/1000 m (The operator of the mine, 2012). The test well drilled in Field-B gave measurements of 85,36 bara at 863 m. That yields a pressure gradient of 9,89 MPa/1000 m. I assume the same pressure gradient applies to Field-A.

According to Triplett, Filippov, & Pisarenko (2001) the mined coal in the area is of low-volatile bituminous(l**vb**) rank. On the other hand, analysis provided by the operator suggest that the coal is ranked towards semi-anthracite. As discussed previously this may influence the success of the project heavily, in terms of permeability primarily. An l**vb**-ranked coal is preferable to a *sa* ranked coal as the fractures may close when coal matures into the anthracitic ranks. I will assume that the coal is of *sa* rank, as a test on the coal provided by the operator must be weighted more heavily than a paper on the coal by an external source.

The gas composition in the coal and surrounding rock is (Corrected for air) 90-98% methane, 0-2,8 hydrogen, 0,1-1,2% carbon dioxide, 1,2-6% nitrogen, less than 1% heavier hydrocarbons and 0-0,265% helium (Triplett, Filippov, Pisarenko, & Blackburn, 2000).

However, the lab report from Field-B states that the gas consist of 99,46 % methane. I find an actual measurement from the area more trustworthy than the values stated in the article, so I will use the value from the lab.

Typically water is present in limestone and sandstone layers, which may act as aquifers, but also in the fracture systems of the coal itself. Water saturation is dependent on depth; below depths of 500-600 m water is usually not present in coals (Triplett, Filippov, Pisarenko, & Blackburn, 2000). If this holds, there are some profound consequences for the profitability of

a CBM project in the area. See figure 1, which show typical production profiles for water and gas for a CBM project. The initial dewatering period puts severe financial strains on CBM projects. If the dewatering period may be avoided, that would be nice. However, since the literature states that the fracture system always is filled with water, I assume that to be the case. If the fracture system show to contain water as (Triplett, Filippov, Pisarenko, & Blackburn, 2000) states, then that will be a nice upside to the project.

Since data on PVT is lacking, both in field-A and Field-B, these must be obtained elsewhere. PVT curves may be generated in Tempest MORE, if the specific gravity of the phases is known. Since the SG is known from the lab, the curves were generated in MORE.

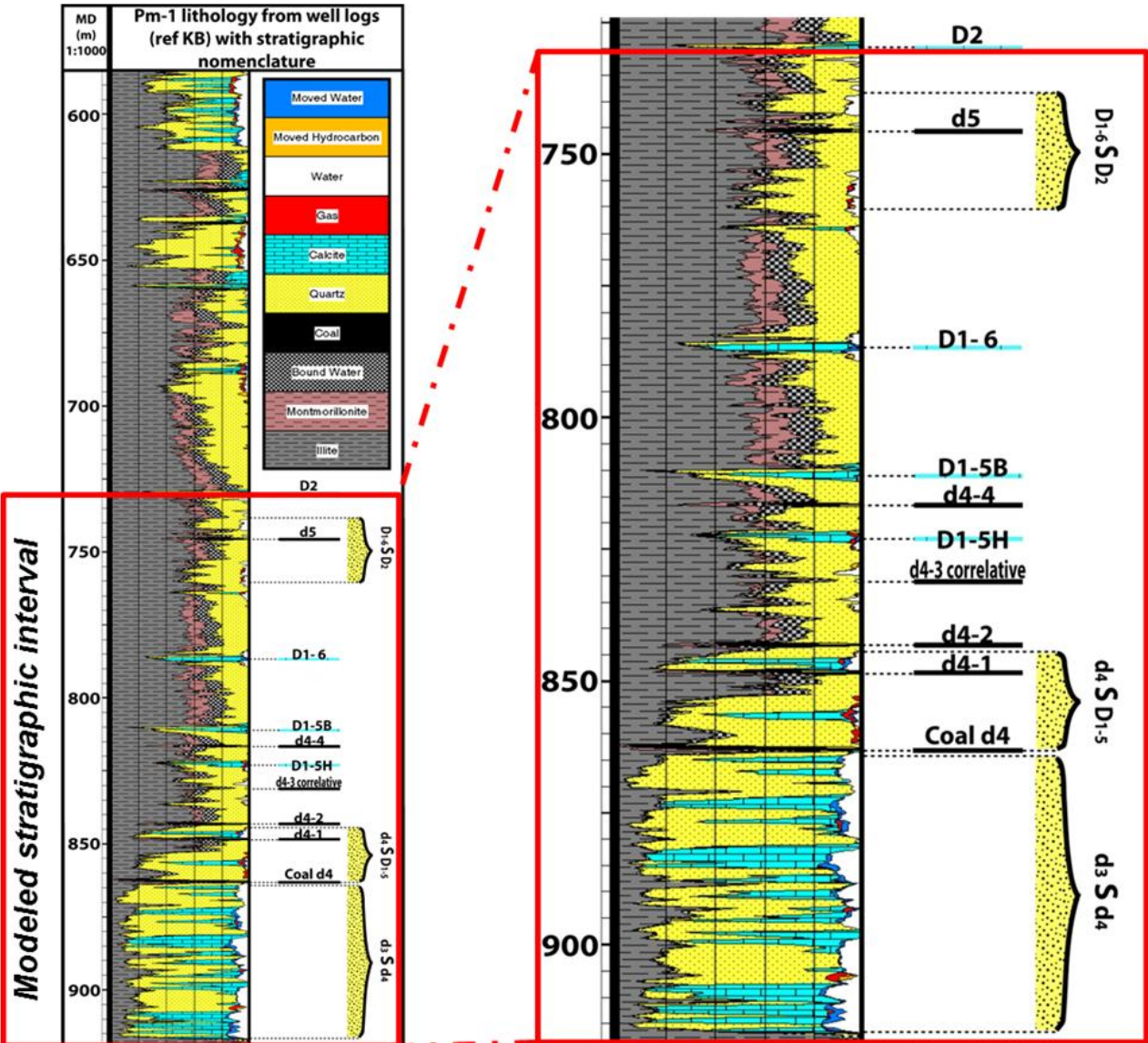


Figure 14: Stratigraphy in the PM1 well in Field-B (Weatherford ASA, 2012).

3 Comparison of Tempest MORE and ECPLIPSE 100 on simulating the Field-A reservoir

The goal of the simulation part is to make two models with the same data, the difference being the software applied. The software used will be Eclipse 100 and Tempest MORE. The objective is to compare the results the different software yields, the input data being the same. To achieve this, a base case was first made, with a single well. Then the permeability and diffusion time was varied, to see how the two models responded to this. Finally, five wells in a fivespot pattern were simulated. This final case also provided some insights as to the feasibility of a project in field-A. But first, a more detailed elaboration on the input data is required.

3.1 A simple one layer, one well model

The goal for this first model was to get a successful run in both simulators using the same data. It was also to see whether the data acquired and/or assumed gives reasonable results, and lastly to see how the field-A reservoir performs.

The structure of the comparison will be a description on the construction and run of each of the respective models, explaining how they work on coal and which data that has been used. Then some concluding remarks on the differences will follow.

3.1.1 Description of Eclipse 100

To simulate coalbed methane in eclipse the add-ons “Coal bed methane” and “dual porosity” are applied. It is not possible to simulate CBM with single porosity in Eclipse 100, but one may do a single porosity compositional simulation in Eclipse 300. CBM simulation is activated by simply writing the keywords “COAL” and “DUALPORO” in the Runspec section. The dual porosity modeling in Eclipse 100 is based on a modified version of the classical paper by (Warren & Root, 1963).

This makes Eclipse work in some unfamiliar ways. The porosity is no longer defined as the fraction of pore volume divided by bulk volume. Instead, it is defined as the ratio of matrix volume divided by bulk volume. Since fracture volumes typically are around 0.1-2% of bulk volume, it is reasonable to use a value of 0.99 for porosity when simulating coalbeds in Eclipse 100. Further, the set of z-cells is doubled in number. This is due to the first half of them being defined by Eclipse as matrix cells, while the other half is defined as fracture cells. Gas may only be stored in the matrix cells, and only produced from the fracture cells. When using the dual porosity and coal option some additional data is required, a table of the Langmuir isotherm must be provided, and values determining the diffusion process through the keywords “DIFFMMF”, “SIGMA” and “DIFFCOAL” must be given. DIFFMMH is a

multiplier which proportionally affects the rate of diffusion of gas from the matrix into the coal. Since this multiplier may be hard to obtain, it is also possible to specify the rate of diffusion using the SIGMA keyword. It is inversely proportional with the “sorption time”, i.e. the time it takes for gas to diffuse from the matrix to the fracture. Such data may be available from a canister desorption test. And indeed, such a test has been performed by (Weatherford Labs, 2012).

One feature with CBM modeling in Eclipse is the possibility of adding a second gas, termed a solvent. This makes it possible to simulate EOR projects in CBM. The injected gas may be either nitrogen or carbon dioxide. This feature will not be used in this thesis, but conversely it may become more used in the future when more CBM projects are in the later stages of production, making EOR more valid.

3.1.2 Description of Tempest MORE and comparison to Eclipse 100

Unlike Eclipse 100 Tempest MORE does not necessarily use a dual porosity model when simulating coal bed methane. This is optional, but it seems that not using it for CBM is most common. Since this paper tries to highlight the differences between the two tools I will use a single porosity model in MORE. In many ways MORE is similar to Eclipse. It offers the user the choice between black oil and compositional simulating, much the same as one may use Eclipse 100 or 300 for the same objectives. A significant difference between the two is that MORE is more user friendly as the editing of the .data file, simulating it and viewing the results may all be done in a single program. In Eclipse, these three processes are separate. Technically, there are some differences as well. I will highlight the ones I encountered for the CBM case in field-A.

Most noteworthy, is the input of the Langmuir isotherm. In Eclipse this is done by giving a table of different pressures which correspond to certain gas storage capacities, which in sum yields the Langmuir isotherm. This is simple, and makes the way from lab results to simulation easy. In MORE it is done differently. There, a set of parameters must be given; Firstly, the volume constant, which controls the volume of gas in the rock, secondly, the Langmuir pressure, which is defined as the half of the pressure where the Langmuir isotherm flattens out, and thirdly, the Langmuir time, which defines how long it takes for the gas to detach from the rock. Together, these parameters define the Langmuir isotherm in the following way:

$$V_l = \frac{P \times V_{el}}{P + P_l}$$

Where V_l is storage capacity in [Sm^3/ton], P is pressure in [Bara], V_{el} is the storage capacity from Eclipse 100 in [Sm^3/ton] and P_l is the Langmuir pressure in [Bara].

To obtain a match in MORE with the table used in Eclipse 100, some tweaking of P_l and V_{el} may be necessary. In figure 39, the result may be seen. A reasonably good match was found, though it seems that the match become inaccurate for pressures exceeding 150 bara. This holds only theoretical consequences as the pressures in this case are significantly lower. But it should be noted, that the two simulators construct the Langmuir isotherm differently, and this will give some difference in the rate of which gas is desorbed from the coal. While the tabular form used in Eclipse 100 is easy to use, it yields little control of how the Langmuir isotherm is constructed. In MORE the reservoir engineer is able to control this construction.

In MORE, CBM simulation, porosity is defined as usual. The fraction entered will be the void represented by the fractures. The matrix porosity is not defined of course, but its storage capability is defined through the Langmuir isotherm, together with the initial reservoir pressure the isotherm defines the gas content of the reservoir. The keyword PDSI, which is initial desorbition pressure, defines when production occurs, as the reservoir pressure must come below its value.

To account for the fact some of the coal is mineral matter, commonly referred to as the ash fraction, and that some of the coal is saturated with water, termed moisture content, the FASH keyword is used. It is simply a fraction, which specifies how much of the coal it is possible to produce from, thus being similar to a normal NetToGross ratio.

Relative permeabilites may be constructed or imported. Normally, rel. perm curves are obtained from the lab, so MORE works much in the same fashion as Eclipse in this regard. The same goes for PVT data, in both simulators it is input as tables and/or keywords.

Regarding the initialization of the model, the simplest way to do it is through initial equilibrium for both simulators. Both simulators allow for arbitrary initial conditions, but that it must be done carefully. I have used initial equilibrium for both simulators.

3.1.3 Simulation input

In this section I will go through the parameters used for the runs, making it easy to for the reader to compare the input with the output of the simulations. I will also give any assumptions I have made, and the reasons to why they were made.

3.1.3.1 The first run: One vertical well

In this first run the goal was to make a simple run in order to calibrate the two simulators against each other, making sure that key parameters such as gas-in-place were the same. After achieving that the goal was to see if there were any differences in the results produced by the two simulators. I hypothesized that differences might come from the fact that the coal option in the two simulators works in some senses, differently, as described in section 3.1.1 and 3.1.2. To test this, it seemed reasonable to make the model simple to get little disturbance from other facets of the simulators that might cloud the result.

Geometry

I've chosen the layer I7 as the object for simulation. It is 1.14 m thick, has a mild dip and lies between 400-800 m below ground. For simplicity I have assumed it to be flat and lying at a constant depth of 600 m. For MORE a grid of 45x45x1 was chosen, making grid size 100x100x1.14 m. In Eclipse 100 a grid of 45x45x2 was needed, to account for the dual porosity.

Permeability

In Eclipse a permeability of 0.0001 mD was assigned to the matrix layer, making it practically tight, and 5 mD in the fracture layer. 5 mD was used throughout the whole grid in MORE. The value of 5 mD is not stemming from a test, but is simply used because it is a typical value for horizontal permeability in coalbed methane reservoirs. Vertical permeability does not apply to this case as it is only one layer.

Porosity

In both simulators porosity was given to be 1%. This is based on what seems to be most typical in the literature.

Temperature

As mentioned the average temperature in the area is 17,6 C at 100 m depth. Since the reservoir is simulated to be at 600 m depth and the geothermal gradient is 2,3 C/100 m the used temperature will be 29,1 C for both simulators.

Relative permeability

The relative permeability curves used are shown in figure 40. They are typical relative permeability curves found in the literature (Karimi & Pinczewski, 2005).

PVT and fluids

From (Weatherford Labs, 2012) the gas composition in Field-B was determined to be 99,46 mol% methane, 0,25 mol% ethane, 0,22 mol% carbon dioxide and 0,08 mol% propane. Based on this I will assume that data for pure methane may be used in the simulation, without too large errors. The specific gravity of methane is 0,5537.

On the PVT behavior of the gas, the assumption that the gas acts as methane is used again. Using the SG of methane MORE calculates the formation volume factor and gas viscosity of a set of pressures. The same data was exported to Eclipse. The data used is plotted in figure 38 in attachments.

Rock compressibility is set to 200×10^{-6} 1/bar for both simulators. This is a huge number for rock compressibility, but history matching studies show that it is appropriate (Roxar, 2012). The value chosen is not based on any data from the field-A or field-B, but is rather a best practice value which is used for these cases. Water compressibility is set to 3.95×10^{-5} 1/bar, which is a value calculated by MORE based on the density and reference pressure given.

Gas content and the Langmuir isotherm

I will use 14,3 sm³/ton as the gas content, as this was the gas content found by (Weatherford Labs, 2012). However, this might be a conservative value, as (Triplett, Filippov, Pisarenko, & Blackburn, 2000) states that the gas content in the field-A mine is around 30-35 sm³/ton. I choose the lab results in this first estimate however, as I consider these fresh lab results as more reliable. In MORE, gas content is put in directly under the Langmuir keyword.

The input of the Langmuir isotherm was described in section 3.1.2, so I will limit the discussion of it here to stating that the original data to construct the table in Eclipse was obtained from the report made by (Weatherford Labs, 2012). The isotherms used may be seen in figure 39 in attachments.

Capillary pressure

Capillary pressure is assumed to be 0. This is an assumption that according to (Roxar, 2012) makes sense for coalbed methane projects as there usually is no significant transition zone between gas and water.

Completion

In both simulators one vertical well was made and placed in the centre of the reservoir. In the well control it was set to a target bottom hole pressure of 5 Bara. The well radius was 0.1905 m. Skin was set to 0.0.

Timespan

In the literature it is stated that CBM wells might live as long as 20 years, or even longer, I've used 20 years as the timespan of the simulations. For reasons that will be given, the timespan of some simulations was extended to 100 years.

Langmuir isotherm

In Eclipse a Langmuir table corresponding to the parameterization used in MORE was used. In both simulators corresponding values for Langmuir time was giving. In MORE the initial desaturation pressure must be given, this was set equal to the reservoir pressure. This was due to practical reasons, as the MORE simulator did not give meaningful results if the value set was lower than the reservoir pressure. This is strange, as it makes it impossible to run undersaturated cases. As to why the simulator cannot handle this, this is not known presently. The support team of Roxar was alerted.

4 Results and discussion of the simulations

In the following section the results that were obtained from the simulations will be shown and discussed. The objective is to show how the differences the two simulators yields from the same input, as well as getting a preliminary look on the feasibility of the projects in field-A.

4.1 Results from the first run and discussion of these

4.1.1 Matching the results from MORE and Eclipse

To get comparable results between the two simulators a lot of effort had to be made to ensure that the input given was equivalent. Though, as described above, the simulators are in many aspects the same, the small differences they have may yield larger differences in the simulator output. As we shall see, the two simulators did not always give matching results, even though the input was as similar as possible.

The first things to do when comparing the output is making sure the initial conditions are the same. A good place to start is the fluids in place. Eclipse yields $226,2 \times 10^8 \text{ sm}^3$ gas, while MORE yields $226,3 \times 10^8 \text{ sm}^3$. This is close. For Eclipse the water in place is $229,6 \times 10^3 \text{ sm}^3$, while MORE yields $228,6 \times 10^3 \text{ sm}^3$. Again, close. Thus, it is clear that initially the fluids in place in the two simulators are close to equal and that the differences in rates we shall see later do not stem from unequal volumes.

In figure 15 the cumulative gas production in MORE and Eclipse is shown. Note two points; First, initially the gas production in Eclipse is rather lower than that in MORE. Of course, the starting dates for both simulators are the same. Secondly, the two simulators diverge at the end of the 20-year period.



Figure 15: Cumulative gas production in MORE and Eclipse.

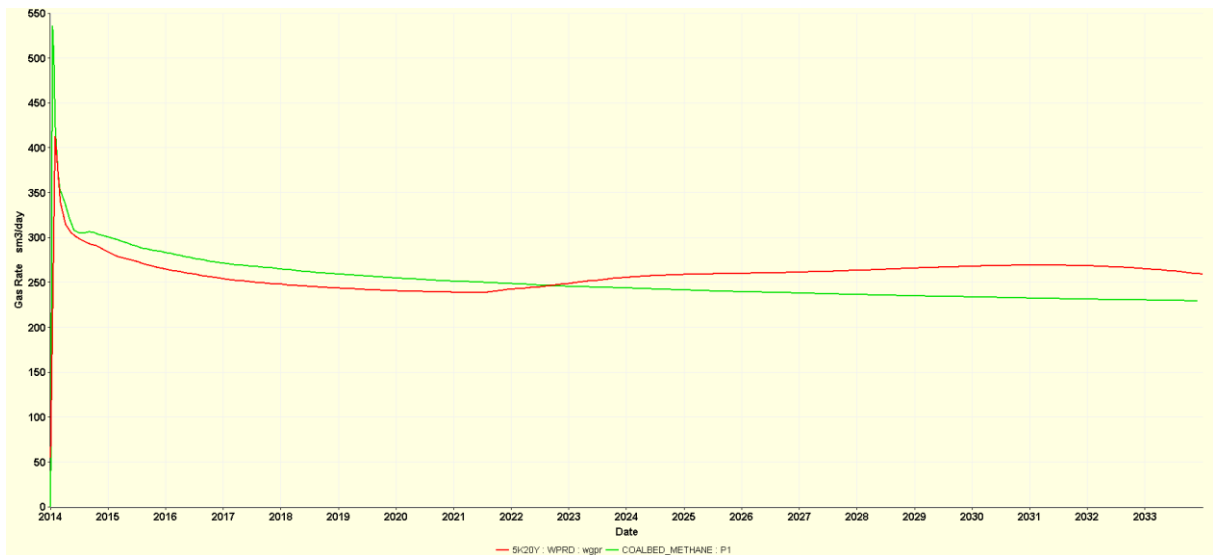


Figure 16: Gas production rate in MORE and Eclipse.

In figure 16 the gas production rate for the two simulators are shown. The two points made on the cumulative production is seen clearer here. The initial spike in production, which would be production of the gas in the vicinity of the well, comes earlier in MORE than in Eclipse. The two simulators show much the same trend until around 10 years into the simulation. An initial spike of production and then a slowing decline. After 10 years of time, the decline continue in Eclipse, while the rate given by MORE increases modestly before it decline slightly again at the end. Comparing to the textbook CBM gas rate example given in figure 1, the curves look unfamiliar. The dewatering period described in figure 1 is not clearly visible, and the spike initially has to short duration to be termed a plateau. The explanation lies in the fact that for these simulations only 1 well is used, while in the textbook examples many are used. This lengthens the dewatering period significantly. So much so, that the

production plateau has yet to come. Later simulations will span a longer period of time, to capture the full behavior of the models.

Noteworthy still, is the discrepancy in production between Eclipse and MORE, which is clear in figure 16. MORE gives higher rates at the end of the 20 year timespan. An explanation for this increase in production might be that the pressure in the reservoir is lower in MORE than in Eclipse, such that more gas is desorbed and later produced. To check if this is the case, some analysis of the pressures in the models was done. In figure 17 and 18, the reservoir pressure in 2023 is shown in Eclipse and MORE, respectively. On visual inspection one may clearly see that the pressure in the areas not being drained by the well is somewhat lower in MORE than in ECLIPSE. This difference quantifies to 0.8 bar, the difference taken in the corner cells.

To further test my hypothesis some cells in the highly depressurized region were chosen for closer investigation. With the origin being in the top right corner, I looked closer on cell 22,32 1, which is at the edge of the depressurized zone, cell 22, 24, 1 which is very close to the well, cell 22,28,1 which is in the middle between the well and the edge of the depressurized zone. The results are given in table 5.

Table 5: Pressure difference in cells in MORE and Eclipse.

Cell	Distance from well	Pressure in MORE [bara]	Pressure in Eclipse [bara]	Difference [bar]
22,32,1	900	58.6	59.2	0.6
22,24,1	100	47.4	47.5	0.1
22,28,1	500	56.3	56.7	0.4

It seems clear that the pressures given by MORE, are generally lower than those given by Eclipse at this time. Further, it is clear that this difference become larger and larger with increasing distance from the well. Thus, this may be the explanation for the gas production rate being larger in MORE than Eclipse at this time. This raises the question: Why does MORE give lower pressures than Eclipse?

No clear explanation is available to me. I see two *possible* explanations. Either the equations used by the simulators are in some aspect different. Such, that the results for coalbed methane simulations always would be somewhat different. But more probable, the differences in how input is given yield differences in the output as well. In MORE the initial desorption pressure must be given, while in Eclipse this is not required. This leaves me without control on ensuring that these are the same. How this initial difference affects the simulations later is not clear, to reveal this a deeper study of the equations behind the simulators would be required. That is beyond the scope of this paper.

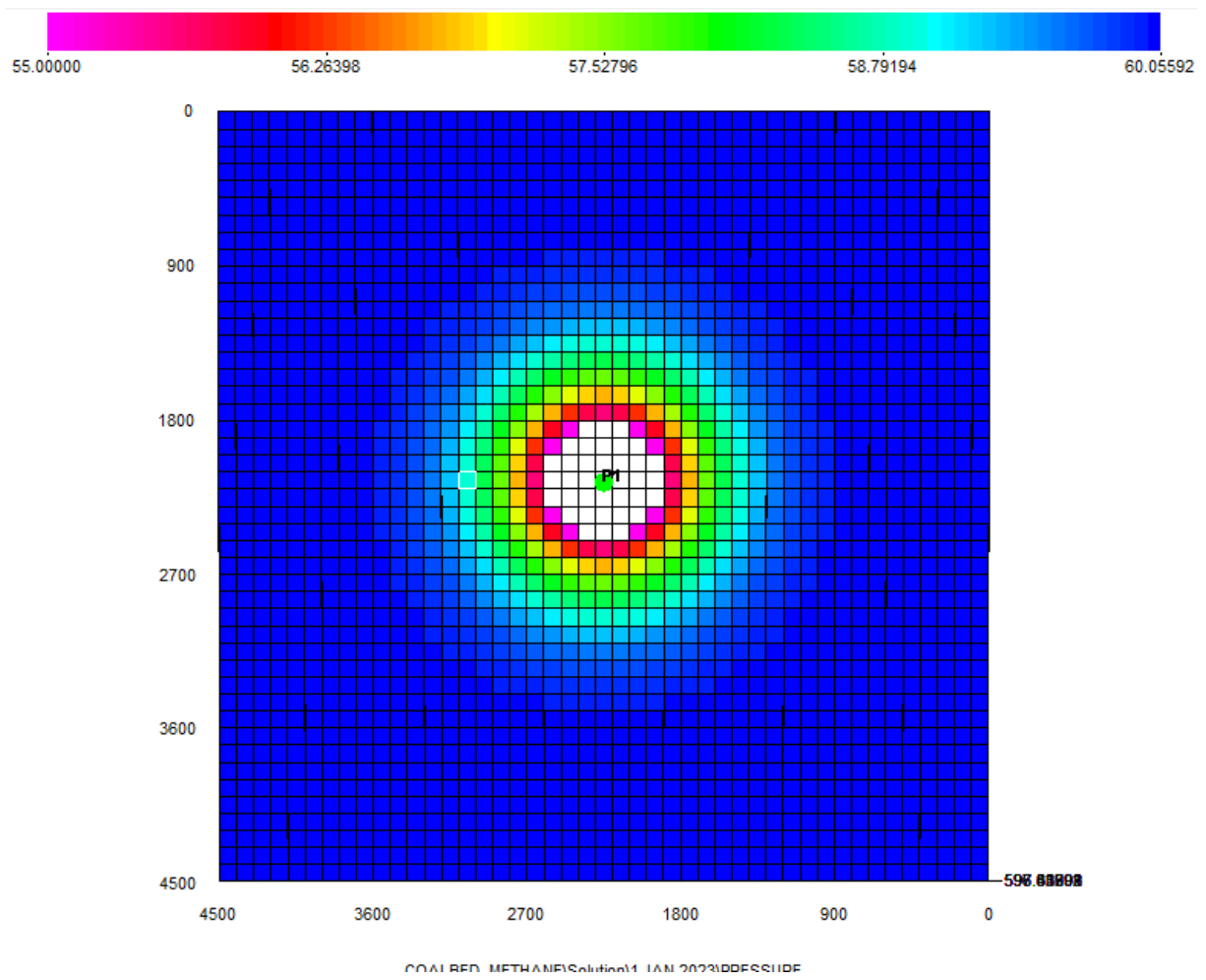


Figure 17: Pressure in the reservoir in Eclipse at 1 January 2023

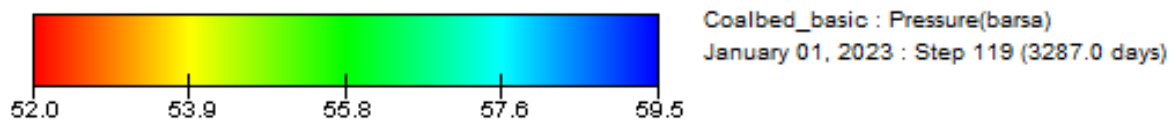
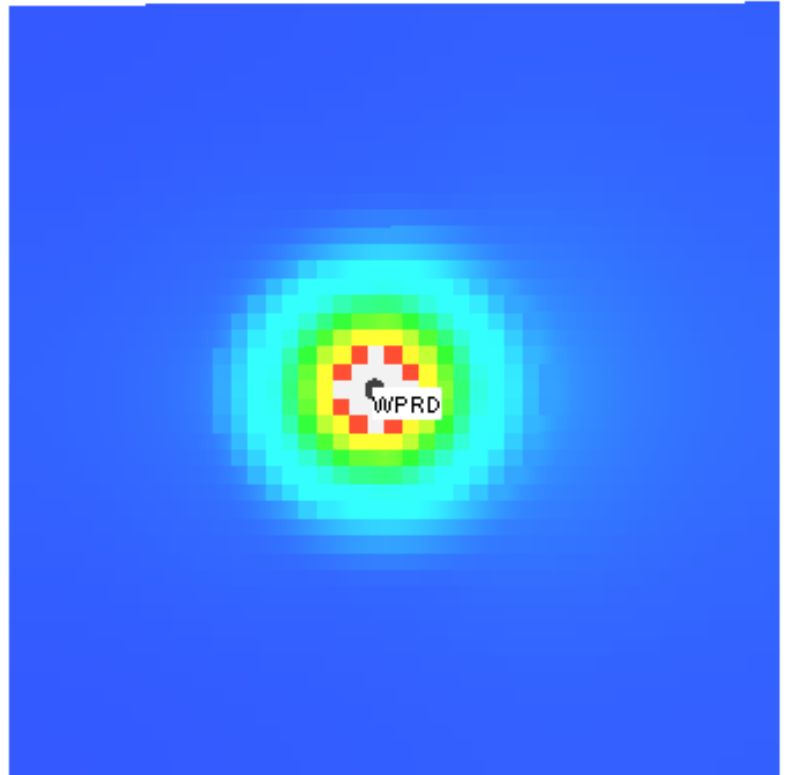


Figure 18: Pressure in reservoir in MORE at 1 January 2023.

Consider figures 19 and 20. They show cumulative water production and water production rate respectively. As with the gas production, MORE yields a higher production of water than Eclipse in the first period of simulation. Unlike with the gas production, MORE yields lower water production than Eclipse at the later stages of the simulation. Looking at figure 20, it is clear that Eclipse yields a higher water production from around halfway through the simulation. This could be explained by the fact that the relative permeability of water is lower in MORE, as the gas saturation in the fracture system is higher in MORE. Which in turn is explained by the lower reservoir pressure, leading to a higher desorption rate of gas.

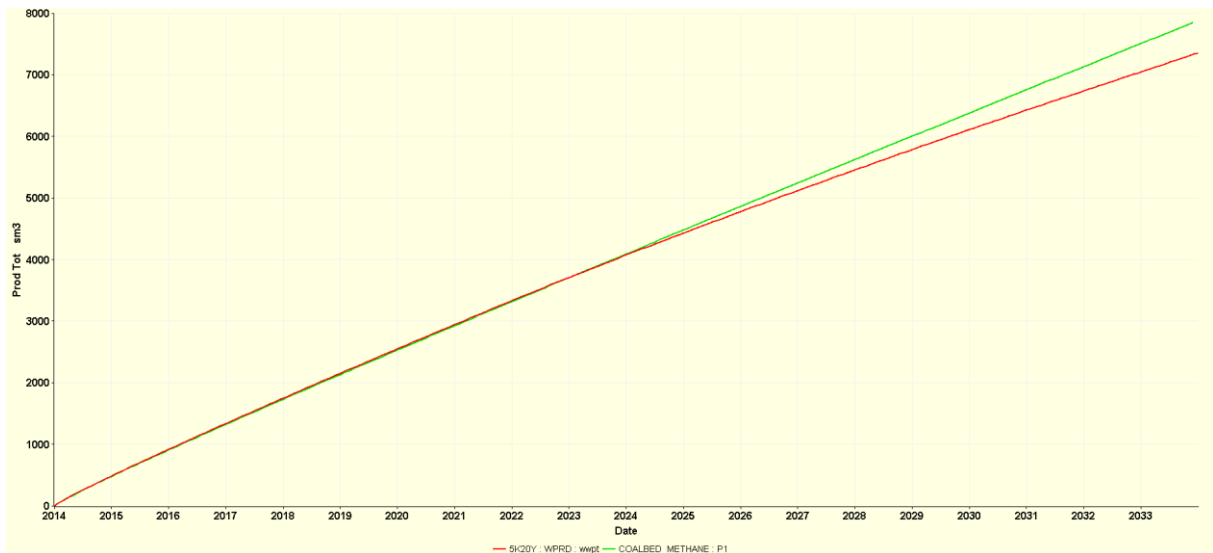


Figure 19: Cumulative water production in MORE and Eclipse.

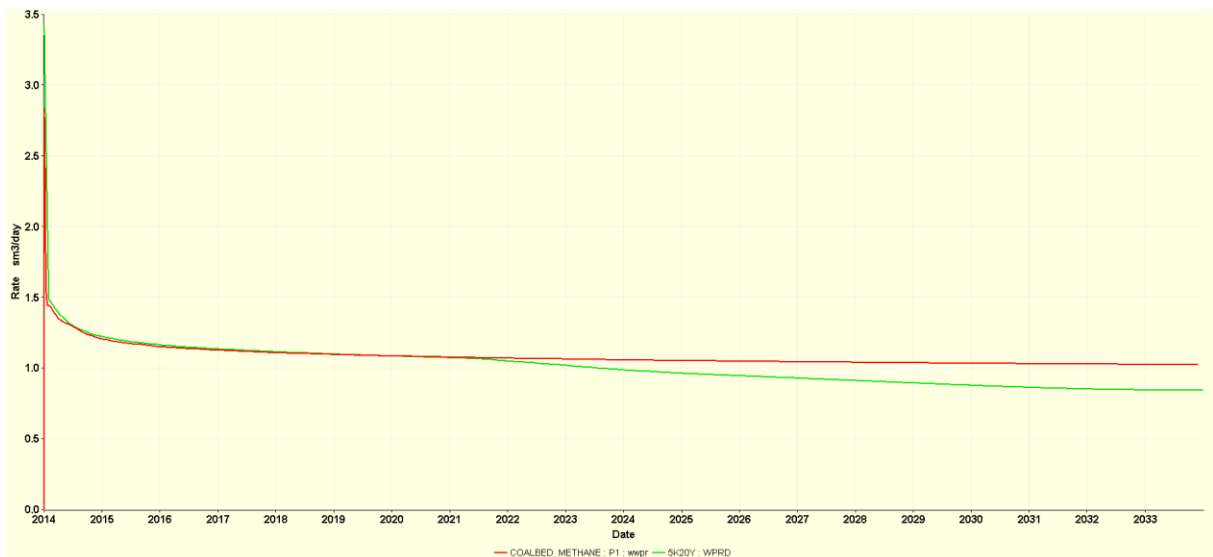


Figure 20: Water production rate in MORE and Eclipse.

Before moving on to sensitivities and longer timespans, some closing remarks on the first run are due. When comparing two different tools, it is essential that the basis for the comparison is proper. As described earlier, all input parameters were as far as possible kept the same, but due to differences in the simulators inputting methods, some parameters could not be input the same way. This is probably why some differences in the output were observed.

The match obtained was in general satisfactory. The fluids-in-place was almost identical and the cumulative production of both water and oil was both quite similar. The water production was a decent match, as both simulators give the same trend, an initial spike followed by a slow decline. It is more troubling then, that the trend in the gas production rate is somewhat different, with MORE giving a rise in production halfway through the simulation, while Eclipse does not. This rise in production was unexpected and therefore the Roxar support was

consulted. This was done to ensure that the simulation in MORE is producing what it should. Support confirmed that the model was functioning as it should, and hence the output difference in the produced gas between MORE and Eclipse must be attributed to the difference in the way input is given, or potentially the equations used.

4.1.2 Sensitivity studies of the first run

To further the understanding of the difference in the two models, some sensitivity studies were made. The parameters that were chosen for change was the horizontal permeability and diffusion time. In the original run these quantified to 5 mD and 2.5 days.

5 mD is a fair permeability in coalbed methane reservoirs (Halliburton, 2007), but not extreme in any sense. Therefore, permeabilities of 10 and 20 mD were used when testing for how sensitive the model is to variance in permeability. These values would be considered high, but as mentioned earlier, permeabilities up to 50 mD has been reported for some cases (Halliburton, 2007), and thus 10 and 20 mD is well within the range of what is possible. The permeabilities that were altered is the permeability in the fractures. To speak of an alteration of permeability in the matrix does not make any sense, as this permeability always is very low, due to the narrow pores.

2.5 days is a short diffusion time (Weatherford Labs, 2012). To test diffusion time's impact on the model, the new values for diffusion time were set to 10, 50 and 100 days.

Studies of permeability

In figure 21 gas (red) and water (green) production rate in MORE is shown. Notice how especially the gas curve looks radically different than in the original run. The gas production rises greatly in the latter 6 years. In the original run, only a slight rise was seen.

The same trend may be seen for Eclipse in figure 22, where gas production rate for $K=20$ mD is shown for both MORE and Eclipse. The two simulators give similar trends, though MORE yield slightly lower rates. So both simulators give a substantial rise in production at the end of the timespan.

Although of little practical importance, it would be theoretically interesting to see where this goes. Therefore the simulation period is prolonged to 100 years, to see how the curve develops. Of course, such a long production period would be unacceptable to an oil company; this is only of academic interest.

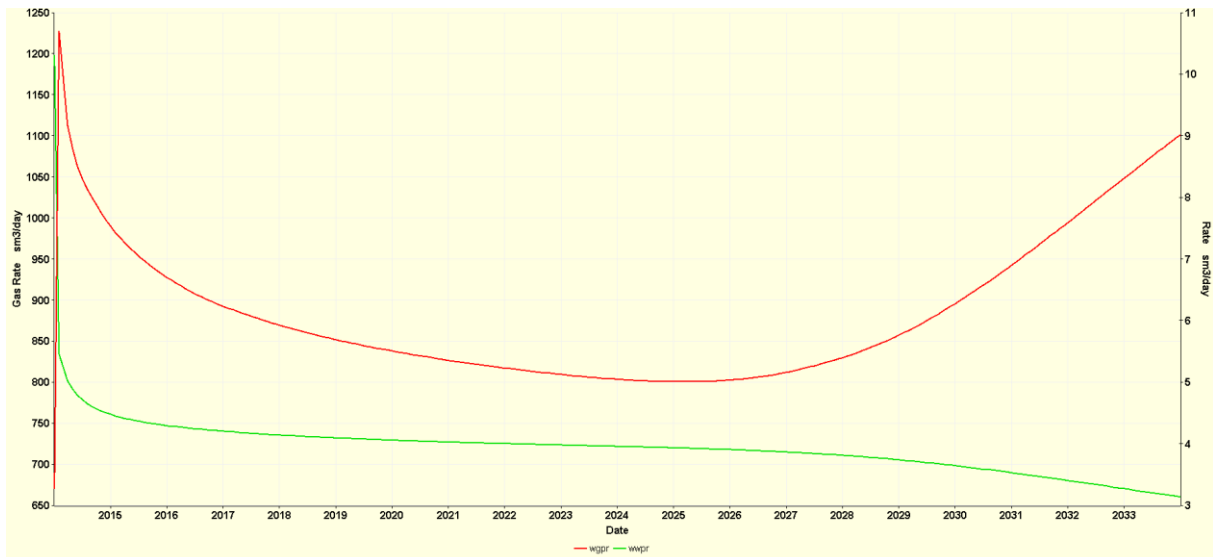


Figure 21: Gas (red) and water (green) production in MORE with $k=20$ mD, 20 year period.

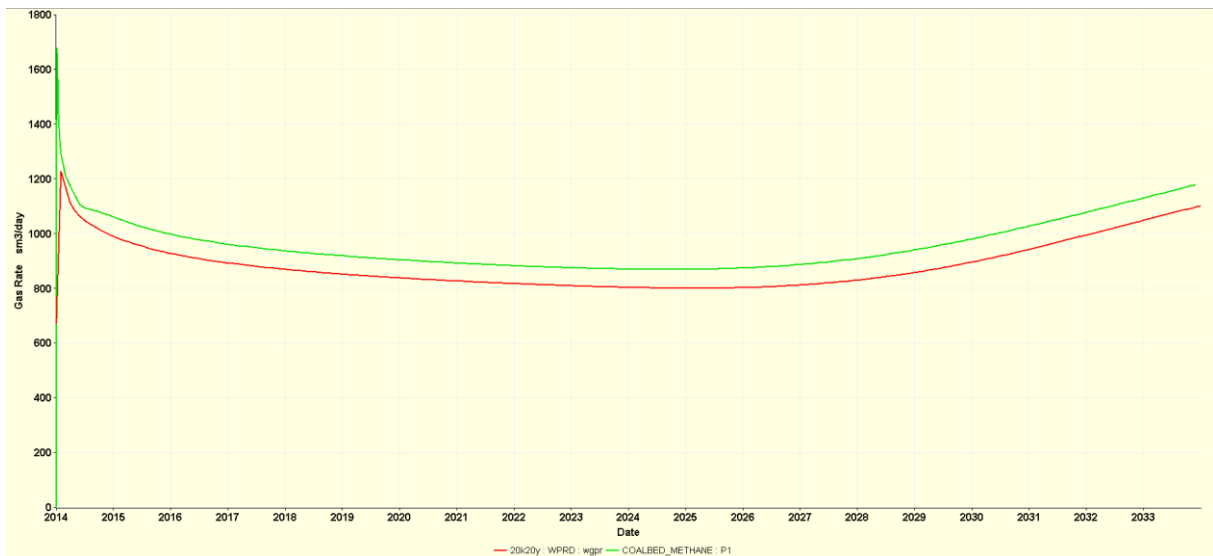


Figure 22: Gas production in MORE (red) and Eclipse (green) for $k=20$ mD, 20 year period

In figure 23 the gas production in MORE with $K=5, 10$ and 20 mD for a 100 year period is shown. The curves are interesting. Notice what happens with the rise observed in figure 21 when the time is extended; It develops into a plateau in year 2065, that's 50 years into the simulation! Then it continues into an expected decline. For the $K=10$ mD the plateau is less sharp, but comes at a later stage, around the end of the simulation. The original run, here extended, does not reach its plateau within the timespan of the simulation. In reality, such long production periods do not occur. The reason that the models display such long periods is that since there is only one well in the model and the permeability is low, the dewatering period and the preplateau period described in the first chapter become extremely long.

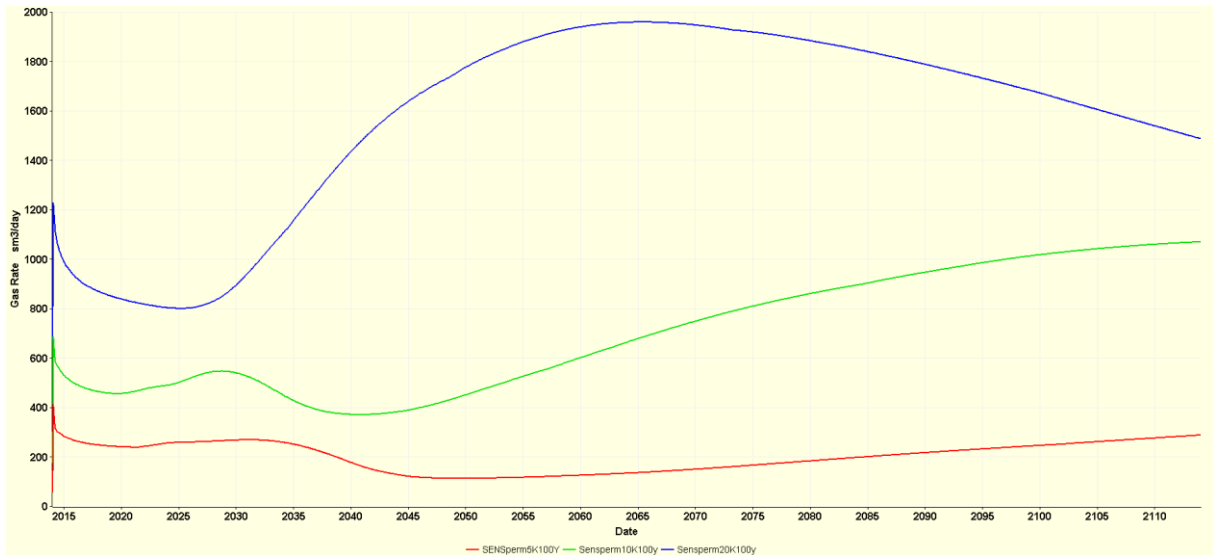


Figure 23: Gas production in MORE with K=5 mD (red), 10 mD (green) and K=20 mD (blue) with simulation period of 100 years.

In figure 23, the gas production rate in MORE and Eclipse for K=5, 10 and 20 mD is shown. As would be expected for such a plot, the curves with similar permeability are close to each other, forming pairs. However, there are large differences between the rates the two simulators produce. And what's interesting is that the value of the difference varies with permeability. Take the 20 mD lines for example; Eclipse yields the larger rates throughout the simulation, especially at the end. While in the 10 mD case the discrepancy is more modest. One would expect a similar discrepancy based on percent for the different permeability runs, but it appears that this is not the case. Comparing the gas production of the plateaus, Eclipse has a 20% higher production than MORE in the 20 mD run, 11% higher in the 10 mD run and 33% higher in the 5 mD run. So, the gap between the simulators is not similar for the different permeabilities, and a clear pattern in the dissimilarity is not clear, as the smallest gap is for the 10 mD run, with larger gaps when increasing or decreasing the permeability.

Also notable, is the minor rise in the production in MORE around 10-15 years into the simulation. This increase is present both in the 5 and 10 mD cases for MORE, but not in the 20 mD case. As mentioned above, this coincides with a minor pressure drop in the model, which explains the incremental production.

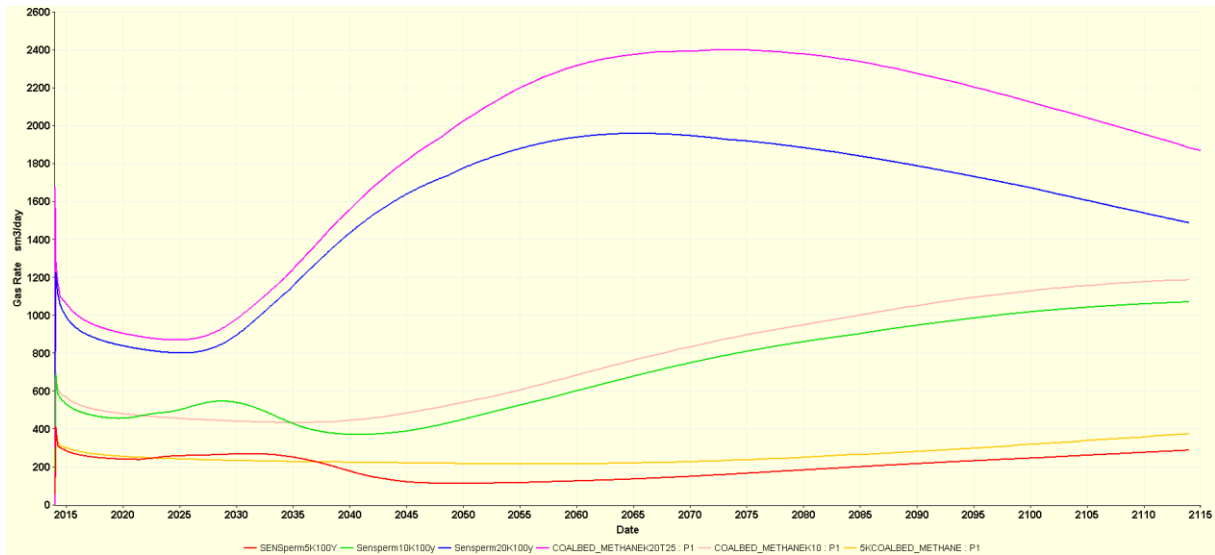


Figure 24: Gas production rate in MORE and ECLIPSE for K=5, 10 and 20 mD. MORE: 5 (blue), 10 (green) and 20 (red). Eclipse: 5 (purple), 10 (brown) and 20 (yellow).

In figure 25, the water production in MORE and Eclipse is shown, for the different permeability cases. Here the discrepancies are much smaller than in the gas production plot. The oscillating behavior of the MORE curves in the 5 and 10 mD cases observed in figures 23 and 24 is also visible here, though in the opposite direction. As discussed earlier, this is due to the relative permeability of water becoming smaller, as the gas relative permeability become larger.

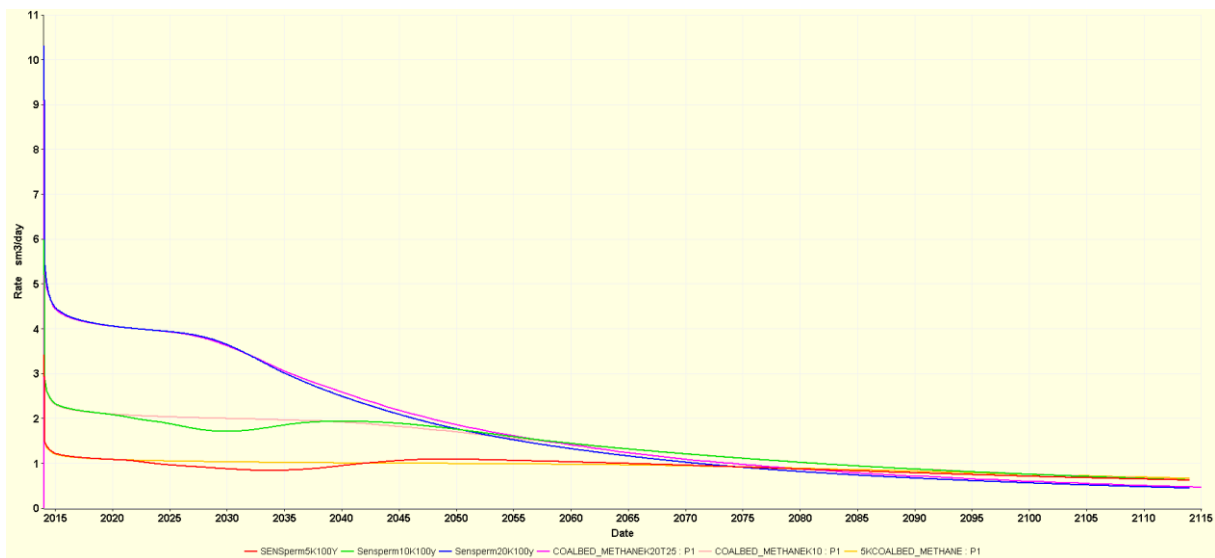


Figure 25: Water production rate in MORE and Eclipse for K= 5, 10 and 20 mD. MORE: 5 (red), 10 (green), 20 (blue). Eclipse: 5 (purple), 10 (brown), 20 (yellow).

Consider figure 26, which show the gas and water production rate for $K=20$ mD in MORE. It looks like the dewatering period could be said to end in around year 2030-2035. That is 17-22 years into the simulation, a typical dewatering time is some months or few years. For a real situation, many wells would be applied and maybe even pumps, to shorten this dewatering period.

The shape of the curve in figure 26 is close to the textbook example. Except for the early spike in gas production the same trend is seen here as in the example in figure 1. A slow rise in gas production as the water production increases. Only after the water production has become low, does the gas production reach its plateau with the normal decline following after.

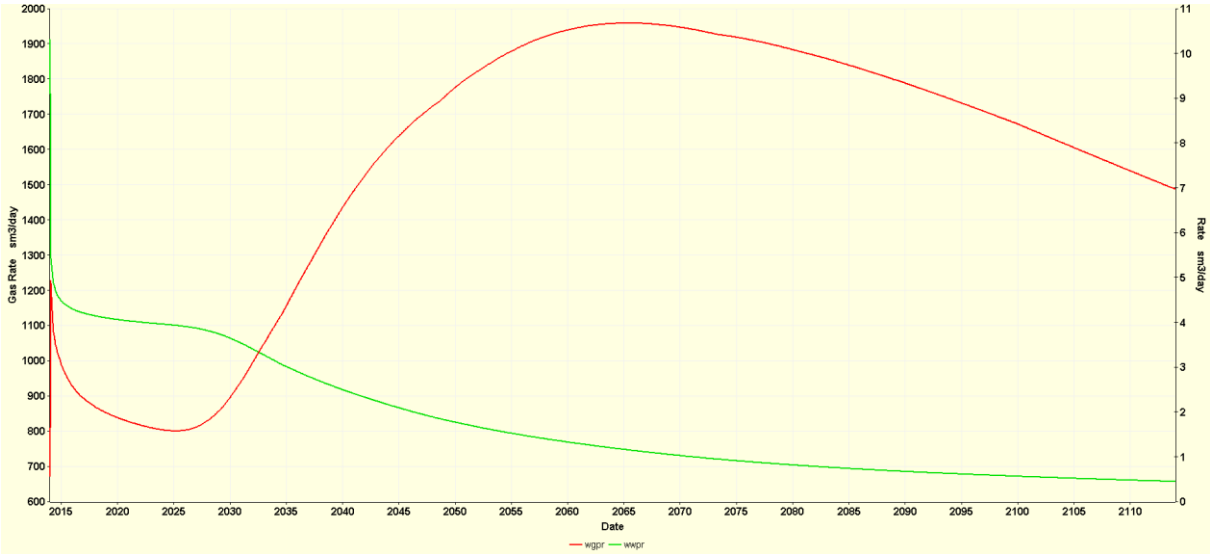


Figure 26: Gas (red) and Water (green) production rate in MORE for $K=20$ mD, 100 year period.

Permeability has a large impact on the production curves. This may be seen in figures 25 and 24 which show the water and gas rates for the different permeabilities, respectively. From darcy’s equation one would expect a doubling of the rate, if the permeability is doubled. However, as Ficks’s law governs the gas when it’s transported from the matrix to the fractures, the picture become more complex.

The simulators, though giving increasing rates with increasing permeability does therefore not abide with this doubling exactly. Not surprising, as there are many more parameters affecting the rates than permeability, but one would assume that they would abide with this roughly. What is interesting about the rates is that the two models do not seem to scale up the gas production equally when increasing permeability. It would be intuitive that if one simulator gave a higher rate than the other at for example 10 mD, then the same simulator would also give the larger rate at 20 mD. And that the difference in rate would be roughly the

same, based on percent. As seen above, the discrepancies were quite different, with 11, 20 and 33 % differences.

To obtain these results, it seems reasonable to think that the simulators use different equations to some extent. Some possible explanations have been ruled out. The transmissibilities used by the simulators are the same, 0.194 in the x and y direction for both. The dual porosity/single porosity should not affect the rates, as these formulations are equivalent (Roxar, 2012). The diffusion times, which as mentioned is input differently, is input such that they should be equivalent. The Langmuir curves input are not exactly equivalent, and may be responsible for some of the difference. The small error in the initial fluids in place will also give some minor error. I do not think the last two error sources stated may alone yield such relatively large discrepancies. Some other difference between the two simulators must be present that I have not managed to find.

Thus, the only sure thing is that at different values for permeability, the difference in rates between the simulators varies. The results seen above, especially in figure 24, are a strong reminder that simulation results are not an absolute truth, but a mere simplification of reality. Two trusted simulators give quite different values with the same input.

Studies of diffusion time

To get the whole picture of how diffusion time affects the model, a permeability of 20 mD was used. The timespan for the simulation was 100 years, in order to capture the full curve of the models.

In figure 27 the gas rates in MORE for the different diffusion times are shown. There are some points to be made. Firstly, it is clear that the diffusion time greatly affects the initial spike in production. As diffusion time gets longer, the spike gets smaller. This is expected behavior as the diffusion time should affect the initial gas production from the closely surrounding area. Further into the simulations MORE give some variations. While the cases for 10, 50 and 100 days give roughly the same production, the original case with 2,5 days give significantly lower production. This is somewhat surprising, as the difference in diffusion should become insignificant in the timespan of such a simulation. Indeed, this is the results Eclipse gives in figure 29, where the gas rates for Eclipse with the different diffusion times are shown. The same behavior on the initial spike is observed in Eclipse, but unlike MORE, Eclipse yields similar production for the different cases afterwards. Care has been taken that no readsorption is allowed in both simulators. Therefore, it is unclear why MORE yields the unexpected result for the 2,5 day diffusion time case. What is clear, however, is that both

simulators perform as expected for the initial spike in production. As mentioned earlier a diffusion time of 2,5 days is considered very short in the literature (Roxar, 2012) (Halliburton, 2007), therefore, by lengthening the diffusion time and thereby decreasing the spiking behavior the gas rate curves look more like the textbook example in figure 1.

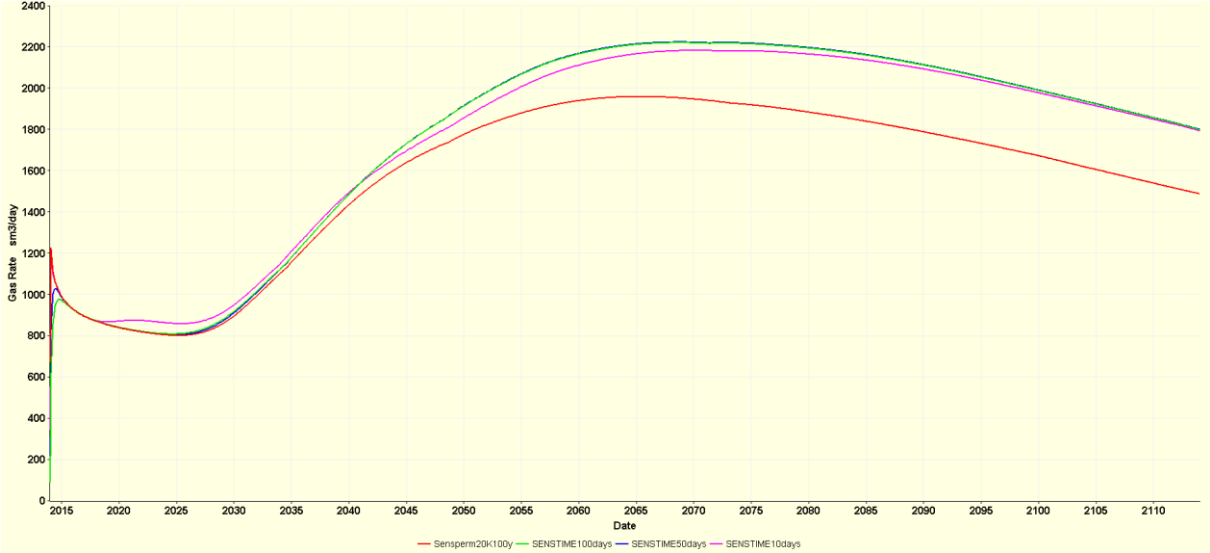


Figure 27: Gas rate in MORE for diffusion time= 2.5, 10, 50 and 100 days.

In figure 28 the water rate in MORE is given for the different diffusion times. The curves are almost exactly similar for all the cases. It can thus be said that diffusion time does not affect water production. As would be expected, as water is produced from the fractures, and diffusion time relates to the matrix. The same behavior was observed in Eclipse in figure 30.



Figure 28: Water production in MORE with diffusion time = 2.5 (red), 10 (green), 50 (blue) and 100 days (purple).

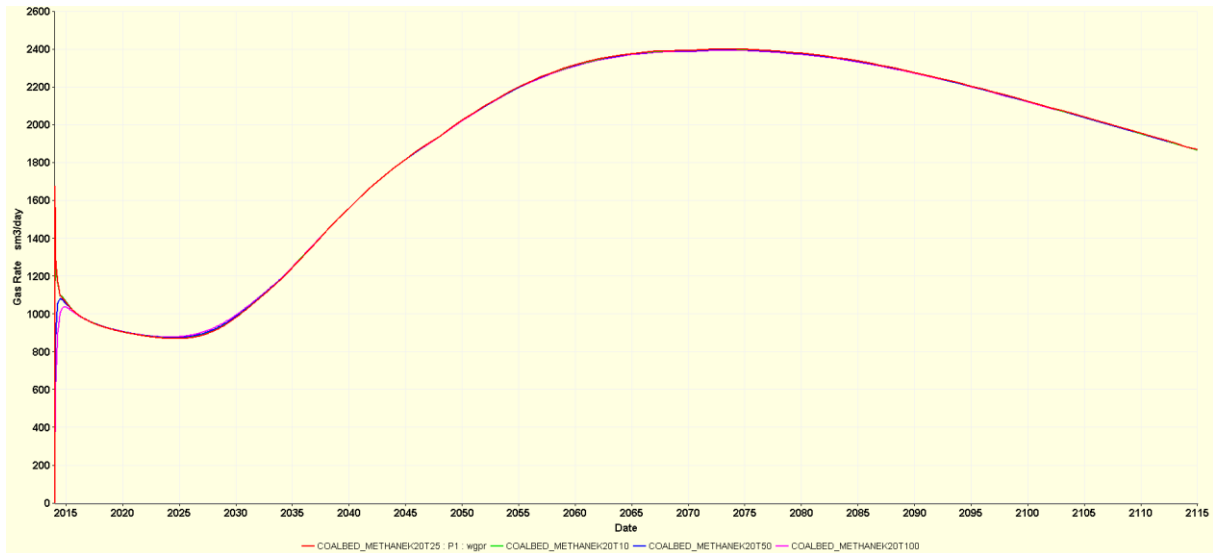


Figure 29: Gas production rate in Eclipse with $K=20$ mD and diffusion times at 2,5 (purple), 10 (blue), 50 (green) and 100 days (red).

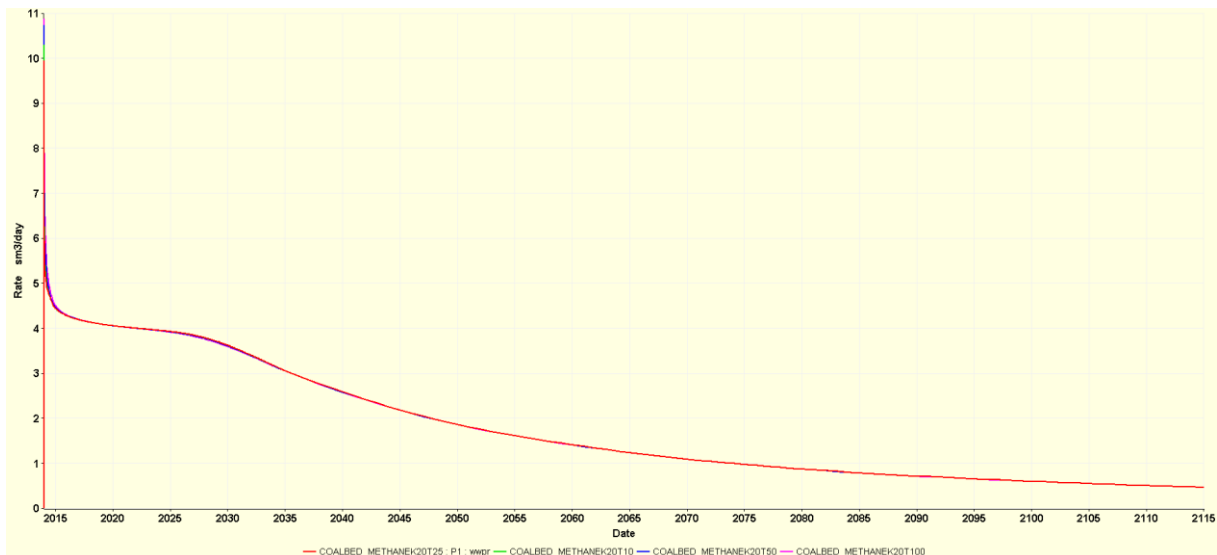


Figure 30: Water production rate in Eclipse with $K=20$ mD and diffusion times at 2,5 (purple), 10 (blue), 50 (green) and 100 days (red).

4.1.3 Simulation of a five spot pattern

Unlike conventional reservoirs, one well's production is increased, rather than decreased by the presence of other wells in its drainage area (Halliburton, 2007). This is explained by the Langmuir isotherm. The further down the pressure is drawn, the more gas is desorbed from the matrix. More wells contribute to draw the pressure down, which all wells benefit from. Also important, closely spaced wells help each other with draining the water together instead of separately as in the single well case. This speeds up the costly dewatering process.

Therefore, well spacing is critical when assessing the feasibility of a CBM project. If the wells are too close, the cost of the wells themselves may ruin the project and if the wells are too far away from each other, the production is lower than it could have been.

In this section, to see how large this synergy effect is, a five-spot pattern model was chosen for simulation. The five-spot pattern is a common well placement technique and is illustrated in figure 31. It should be noted, that normally, in a fivespot pattern the middle well is an injector. This is not the case here; all the wells are producers.

Such simulation was done both in MORE and Eclipse, with $K=20$ mD and the timespan is 100 years. 300-500 m is typical well spacing in CBM projects. In the models in this report, the distance in x- and y- direction was 300 m, making $r=424$ m.

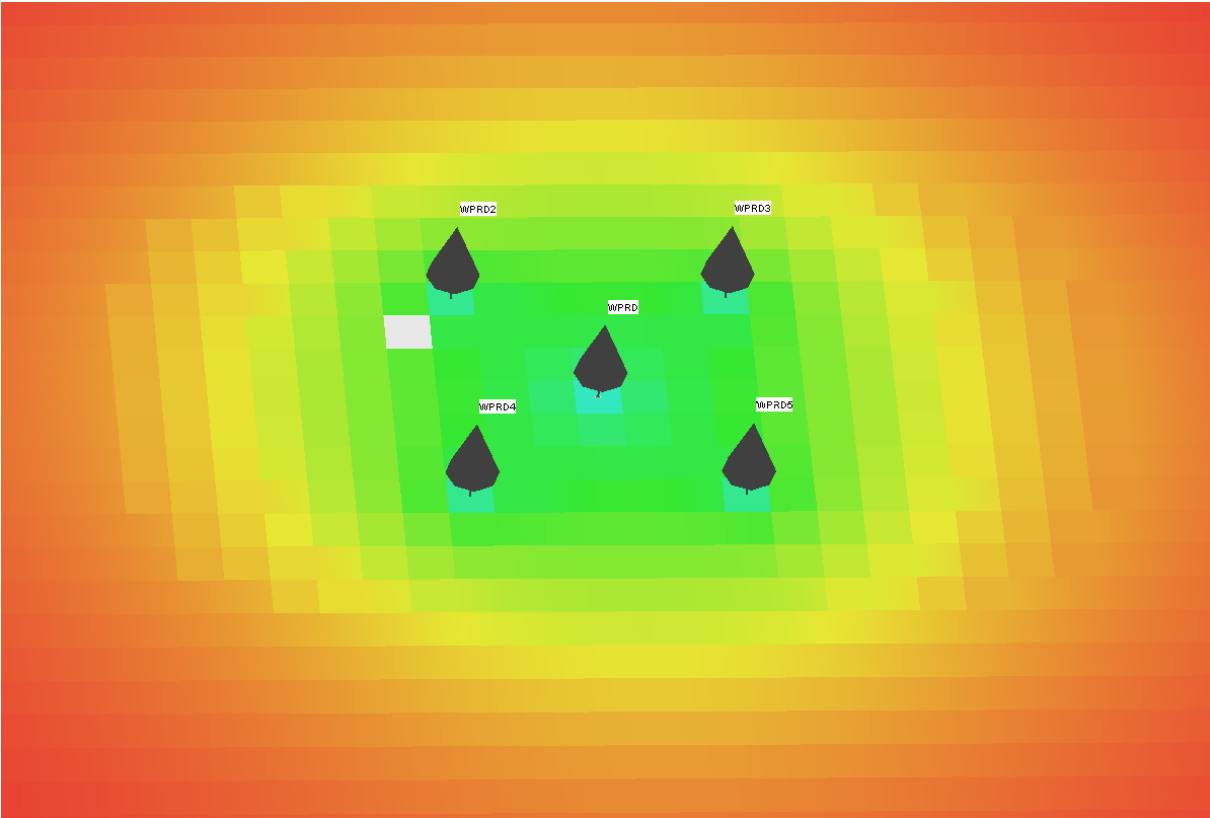


Figure 31: Screen shot of the five-spot pattern model in MORE.

In figure 32 gas production rate in Eclipse is shown, for the five-spot pattern case. There are five wells; P1 (red) is the one in the center. P4 and P5 are hidden beneath P2 and P3 and are not visible, but performing similarly as the two others, as they should, as they are placed symmetrically around P1. The synergy effect of closely spaced wells is visible in figure 32. The P1 well has much larger production initially than the others, as it should, as the water in its drainage area is drained faster with the help of the other wells. The pressure is lowered faster as well, increasing early desorption from the matrix, and thus gas production. The same observations may be made in MORE in figure 33, where gas production rate is shown for a five-spot pattern for all the five wells.



Figure 32: Gas production rate in Eclipse for a five-spot pattern. The wells are P1 (red), P2 (green), P3 (blue), P4 (purple) and P5 (yellow).

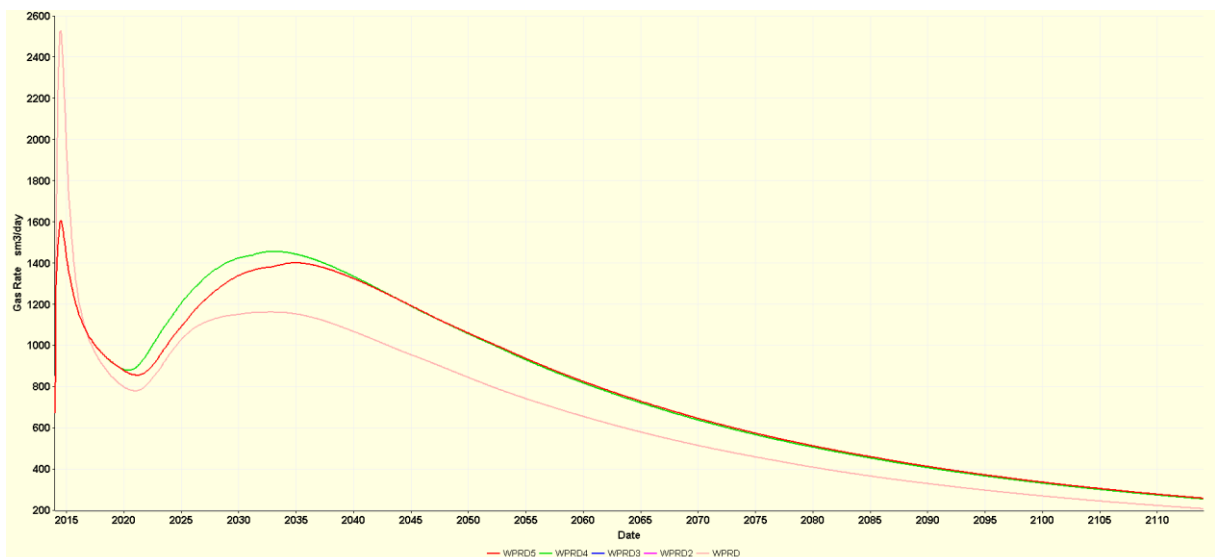


Figure 33: Gas production rate in MORE for a five-spot pattern. The wells are WPRD (red), WPRD2 (green), WPRD3 (blue), WPRD4 (purple) and WPRD5 (yellow).

In figure 34 the gas production rate of the five-spot pattern cases in Eclipse and MORE is shown together with the corresponding single well cases. For the five-spot cases, Eclipse and MORE give quite similar curves, the trend being the same throughout the simulation.

The effect of adding wells is clear. Firstly, the initial spike in production is far larger for the five-spot pattern cases. And it lasts longer as well. Further, the plateaus of the five-spot wells are shifted around 35 years ahead in time. Also, the five-spot wells produce less gas in total compared to the single wells, as they share drainage area with neighboring wells while the single wells don't. This shows the clear synergistic effect that closely spaced wells have on

CBM projects; the production is shifted earlier in time, which is important to the cash flow of a project.

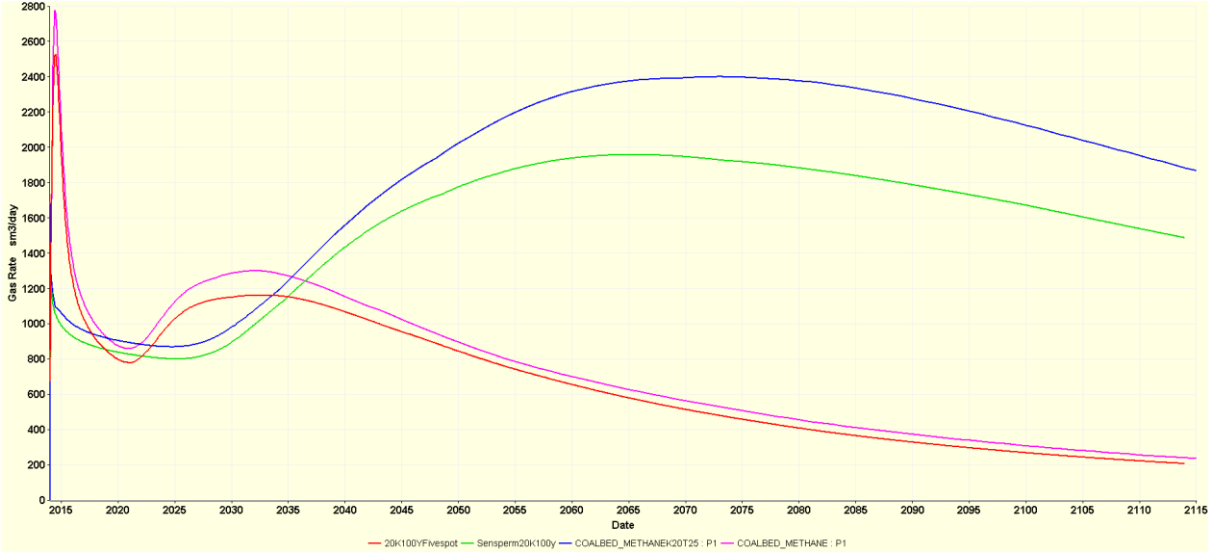


Figure 34: Gas rate for the center well in a five-spot pattern for MORE and Eclipse, shown together with the corresponding single well cases. Five-spot MORE (red), Single well MORE (green), Five-spot Eclipse (blue) and Single well Eclipse (purple)

The effect of the water produced from the center well may be seen in figure 35, where it is shown for both MORE and Eclipse for both five-spot pattern cases and single well cases. The trend is clear; the five-spot pattern cases yield much lower water production than the single well case. This is because the neighboring wells produce much water in the five-spot case, such that the center well does not produce as much. It is this effect, which together with the higher depressurization, leads to the higher early production for the center well in the five-spot case.

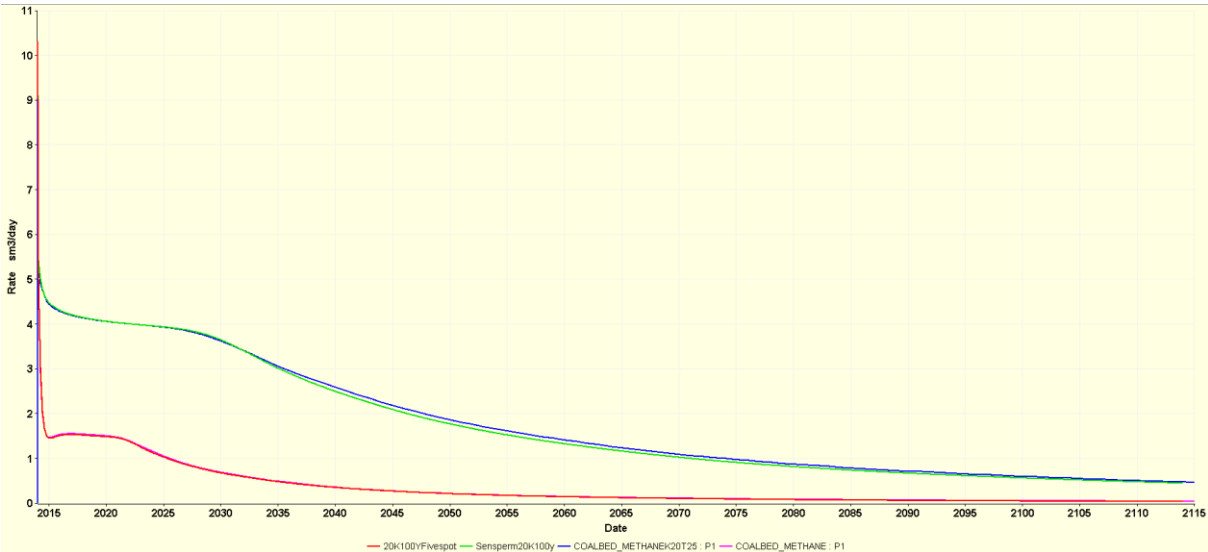


Figure 35: Water production rate for center well in MORE and Eclipse for five spot pattern and single well. MORE five spot (purple), MORE single well (blue), Eclipse five spot (red) and Eclipse single well (green).

4.2 Feasibility of field-A as a Coalbed methane project

Now to assessing the feasibility of a coalbed methane project in field-A. The simulations above have some clear limitations as tools of evaluating the feasibility of the project. Firstly, there is the number of wells. In a realistic scenario, the distance between wells would be 300-400 m, throughout the reservoir. That would mean around 80 or more wells for the 20 km² reservoir I have used. As seen in the chapter on simulation with a fivespot pattern, the synergistic effect of adding wells is very important in ensuring that an acceptable rate of gas production is achieved from early on. These effects are vital, so making profit calculations with the one-well scenarios is quite meaningless. Therefore, the fivespot case was chosen for the profit calculations.

There is also the issue of permeability. As stated earlier, no data is available on permeability for the Field-A reservoir. Therefore, a best guess based on the literature I have encountered during this thesis was performed. The first guess of 5 mD is conservative, and it is probable that the permeability is that or higher. The 10 mD is more optimistic, but still inside the range of what is quite usual. The 20 mD guess is quite optimistic. Although permeabilities of up to 50 mD have been reported in the US (Halliburton, 2007), it would be lucky if field-A turned out to have a permeability of 20 mD. In my simulations, as I have used few wells, it is the case that in order to see the plateau within a somewhat reasonable timespan, the permeability must be high. Therefore I will base my assessment on the 20 mD case of the fivespot pattern.

Since typical coalbed methane wells have a lifespan of around 20 years, this timespan was used when calculating profitability. In order to get a first estimate of the profitability some assumptions were made; A fixed gas price of 0.45 \$/Sm³, a total well cost of 850 000 \$ pr. well, 0.5 \$/Sm³ cost of water disposal, 0.04 \$/Sm³ cost of treating gas. These assumptions were based on similar CBM projects done by Weatherford Petroleum Consultants. Regarding the costs of treating the gas and water, these assumptions should be reasonably safe, as the cost arise from equipment and manpower. More uncertain is of course the gas price, which depends on a number of variables. I will not do any speculation on future gas prices here. The cost of the well is for a vertical well without stimulation, and is thus applicable to the case in question. However, there will always be uncertainty related to the final well cost, as problems might be encountered during drilling, thus extending expensive rig time. Also, the wells might need stimulation, in order to perform as well as assumed from the simulation. Thus making the uncertainty of the well cost the same as the uncertainty of the permeability.

It should also be noted, that the following profitability analysis does not take into account a number of key parameters, such as: Tax, downpayment of debt (which usually is required), depreciation of assets (due to debt) and probably several more. Such an analysis is outside the scope of this thesis. The following simple analysis will serve as a discussion point.

In figure 36, the cumulative cash flow of the fivespot pattern case in Eclipse and MORE with K=20 mD is shown.

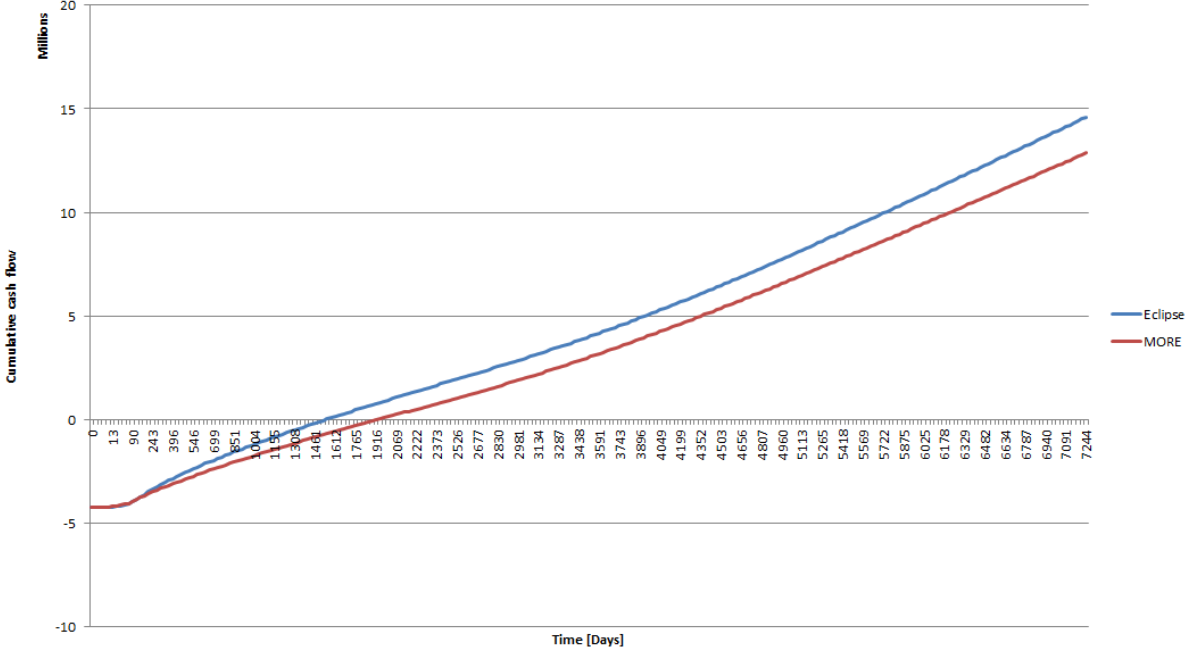


Figure 36: Cumulative cash flow for fivespot pattern case from Eclipse (blue) and MORE (red) with K=20 mD with a timespan of 20 years

There are some points to be made. Firstly, the two graphs both start at -4250 000 USD, which is the cost of the five wells. Then there is period of time until the cumulative cash flow of the project become positive. Due to its higher rate, the scenario from Eclipse breaks even first, at around 1500 days, or around 4 years. MORE breaks even at around 1800 days, just shy of 5 years. Then cash flow accumulates further for both simulators until they end after 20 years. Eclipse yields almost 15 MMUSD and MORE almost 13 MMUSD. I think the conclusion that may be drawn from this is that it is well possible that a CBM project *may* produce enough gas to make it economic, but, that it strongly depends on the permeability being favorable and that the costs are kept low. Further investigation should therefore be done on the permeability to see if this is sufficiently high, and if not, how expensive and effective stimulation would be.

5.0 Conclusion

A literature study has been done on coalbed methane. I found that knowledge of coal rank is essential when looking to do a coalbed methane project. That is due to it defining the coals ability to generate and retain gas, its permeability and how much moisture that may be present. As coalbed methane projects often may have only marginal profitability, good knowledge of coal rank and the mentioned parameters is key. Permeability may be the most critical, as it is often too low to yield commercial rates. The simulations that have been done have shown the impact of permeability. The difference in gas rates between the 5, 10 and 20 mD cases was large. In order to obtain satisfactory permeability, stimulation of wells may often be necessary.

This thesis have highlighted that simulations are a mere simplification of the real world. It is striking when two trusted simulators take the same data but yield different results. The trends the simulators showed were similar in all cases, but the values they gave were different. For the permeability variation study they were highly so. The differences the simulators produced must be attributed to the inherit differences in the solutions they utilize. I have shown how the mode of input into the simulators is not always the same. The input of the Langmuir isotherm serves as a good example. However, this difference, together with the other input differences should not yield the large output differences that were observed in some of the cases above. That is due to the discrepancy between the Langmuir isotherms being relatively modest, the same goes for the discrepancy between the initial fluids in place. This leads to the conclusion that there must be some mathematical difference between the models; that the differences arise in the calculations, not due to the input. For further studies, I would recommend a deeper investigation into the mathematics in order to determine just how the differences in output observed in this thesis arise.

On the feasibility of field-A I found that only the fivespot model could be used to assess the project. This was due to it being the only one of the models in this thesis that captured the synergistic effects that multiple wells closely situated yield. The synergistic effects are the shortening of the costly dewatering time and increased gas desorption. However, as the fivespot model only have 5 wells, while the real field would have at least 80, the application of the fivespot model as a tool of project evaluation is limited. The conclusion on feasibility must therefore be somewhat careful. I think the fivespot model show that it is well possible to produce enough gas in field-A for the project to be economic, but that strongly rests on a high permeability and keepings costs down. Prior to the projects go-ahead, a more detailed economic analysis, incorporating the tax regulations of the area, debt and other expenses omitted here must be done.

List of symbols used

A = Area

C = Temperature, Celsius

C_m = matrix gas concentration

$C(p)$ = equilibrium concentration at matrix-cleat boundary.

D = diffusion coefficient

mD = Permeability, milliDarcy

k = Absolute permeability

K = Absolute temperature, Kelvin

L = Length

m = Length, meter

q_{gm} = Gas production rate from the coal matrix

P = Pressure

P_{ds} = Desorption pressure

P_L = Langmuir Pressure

ΔP = Pressure difference between two points

Q = Flow rate

S_f = fracture spacing

μ = Viscosity

V = Volume

V_l = Langmuir Volume

V_m = matrix volume

\AA = Length, Ångström

Bibliography

- Forster, P., V. Ramaswamy, P. Artaxo et. al (2007). *Changes in Atmospheric Constituents and in radiative forces*. Cambridge: Cambridge University Press. Cambridge, United Kingdom and New York, NY, USA
- Rogers, Rudy. E, Halliburton. (2008). *Coalbed methane Principles and Practices, Third edition*.
- Karimi, K., & Pinczewski, W. (2005). *Coalbed methane reservoir simulation studies. The university of South Wales*.
- Palmer, I. (2009). *Coalbed methane completions: A world view. International journal of Coal Geology*. Higgs-Palmer Technologies, Albuquerque, USA
- Roxar. (2012). *MORE Technical References*.
- Rushing, J., & A.D. Perego, A. P. SPE, Anadarko Petroleum Corp. and T.A Blasingame, SPE, Texas A&M University (2008). *Applicability of the Arps Rate-Time Relationships for Evaluating Decline Behavior and Ultimate Gas Recovery of Coalbed Methane Wells. Presented at CIPC/SPE gas Technology Symposium 2008 joint conference held in Calgary, Alberta, Canada, 16-19 June 2008*.
- Sachsenhofer, R., & Privalov, V. (2011). *Basin Evolution of the **Field** basin (Ukraine, Russia): Implications for CBM potential*. Adapted from oral presentation at AAPG European Region Annual Conference, Kiev, Ukraine, October 17-19, 2010
- Sachsenhofer, R., Privelov, V., Zhykalyak, M. et al. (2001). *The Donets Basin (Ukraine, Russia): Coalification and thermal history. International journal of Coal Geology 49*.
- Salsberry, J. L., Schafer, P. S., & Schraufnagel, R. A. (1996). *A guide to coalbed methane reservoir engineering. Gas research institute. Chicago, Illinois, USA*.
- Triplett, J., Filippov, A., & Pisarenko, A. (2001). *Coal mine methane in Ukraine: Opportunities for production and investment in the **Field** coal basin*.
- Triplett, J., Filippov, A., Pisarenko, A., & Blackburn, S. (2000). *Coal mine methane recovery in Ukraine: Business plan for a development project at **field-A***.
- Warren, J., & Root, P. (1962). *The behaviour of naturally fractured reservoirs*. spe 426. Gulf research and development co. Pittsburgh, P.A.
- Weatherford ASA. (2012). *End of Well report, PM1, **field B***.
- Weatherford Labs. (2012). *Final Reservoir assesment report, **field-B** PM-1*. Trondheim.
- **The terms highlighted in Bold writing, like “field”, “field-A” and “field-B” have been edited such as too maintain discretion to the operator of the field.**

Attachments

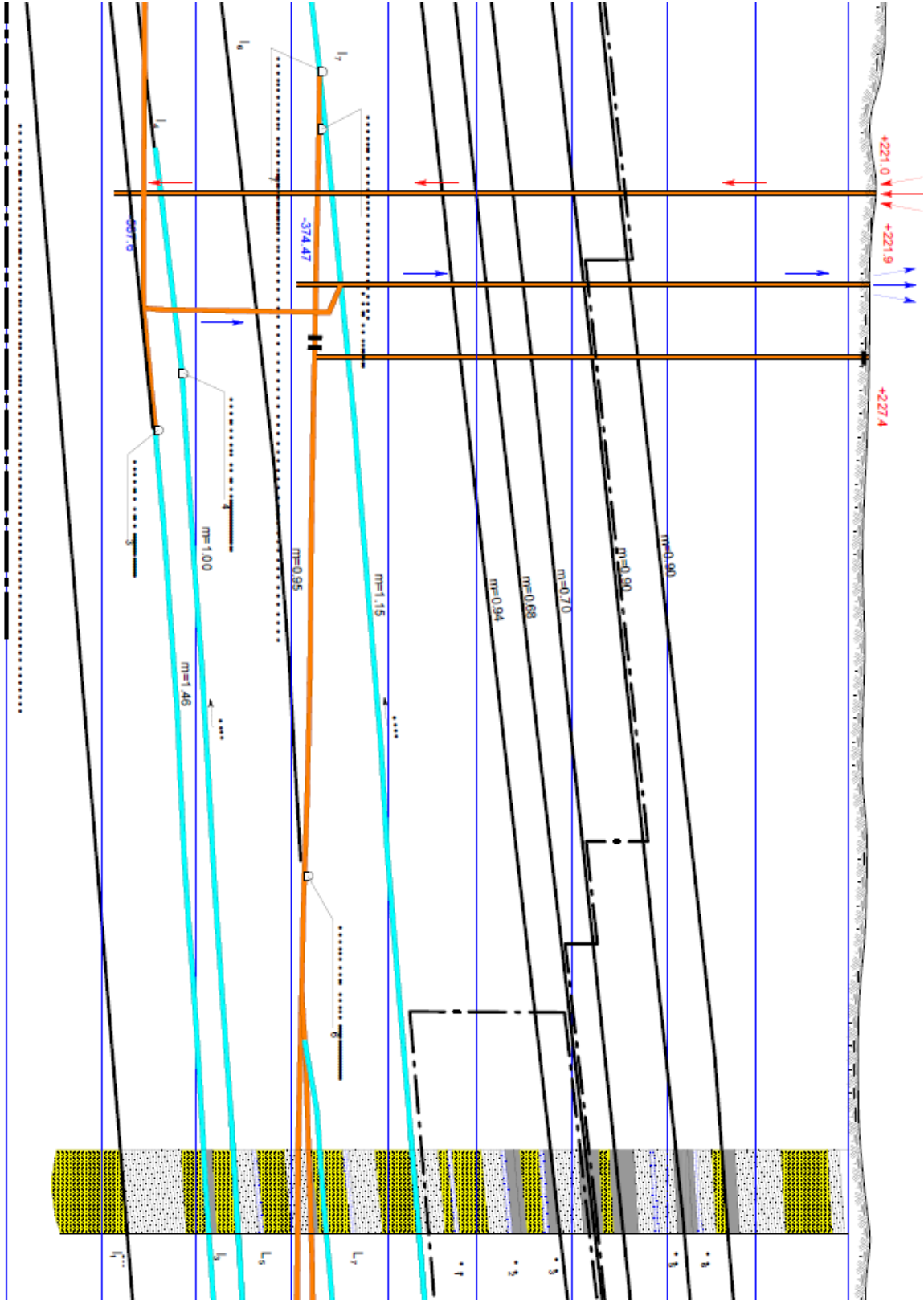


Figure 37: Coal layers with depths and thicknesses in the Field-A mine. From (DTEK, 2012).

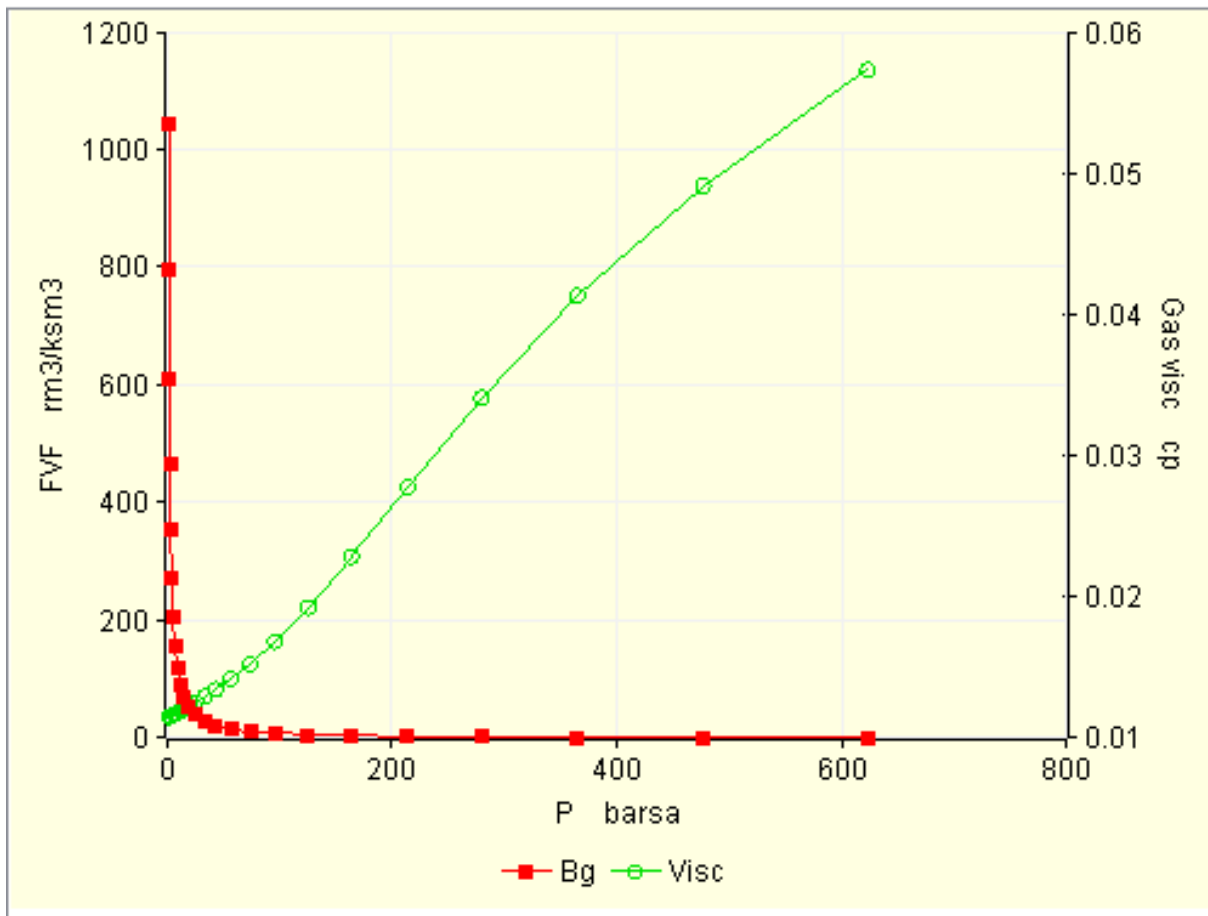


Figure 38: PVT data generated and visualized in MORE.

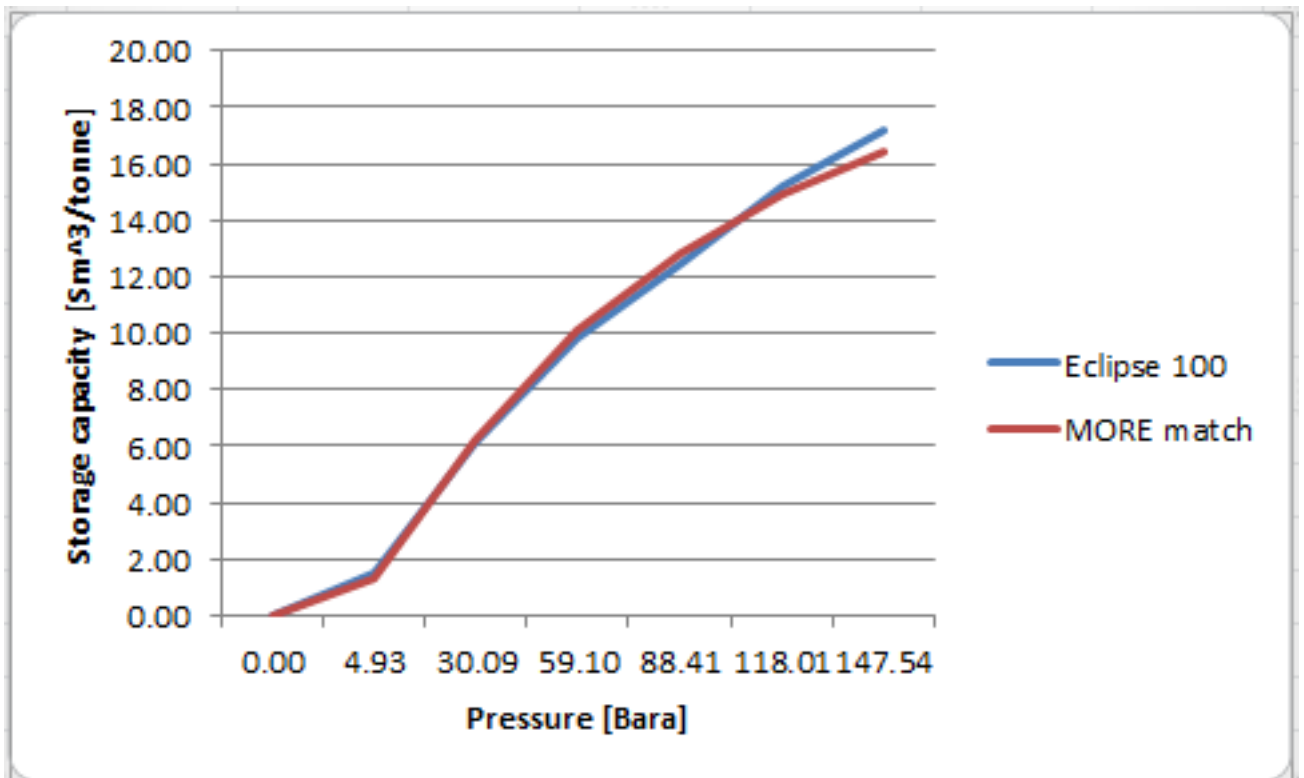


Figure 39: Matching of the langmuir isotherms.

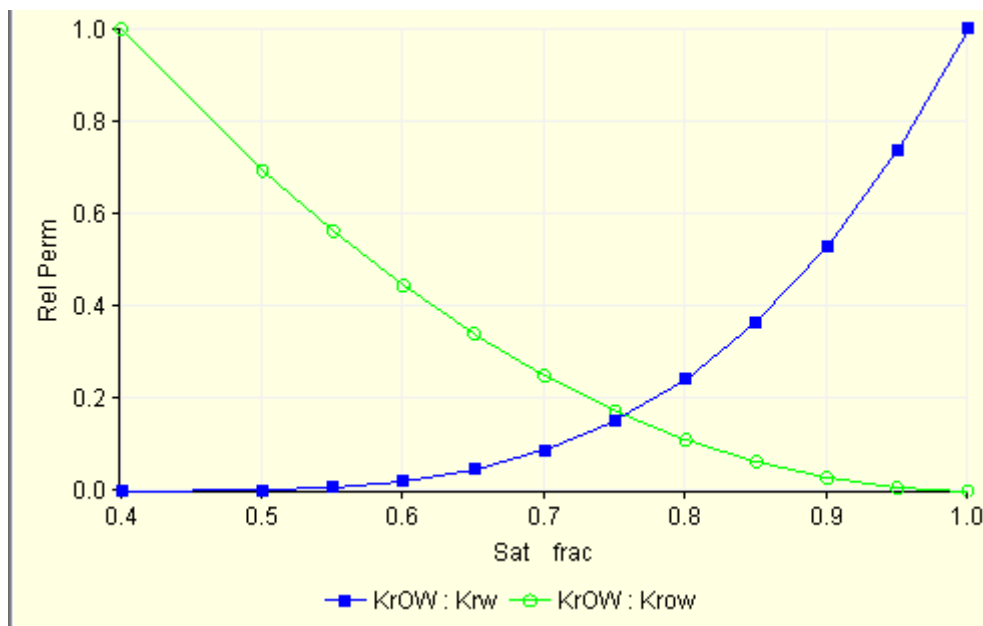


Figure 40: Relative permeability curves used in simulation. Visualization done in MORE.